Dear author,

Please note that changes made in the online proofing system will be added to the article before publication but are not reflected in this PDF.

We also ask that this file not be used for submitting corrections.

Cretaceous Research xxx (xxxx) xxx

Contents lists available at ScienceDirect

Cretaceous Research

journal homepage: www.elsevier.com/locate/CretRes

Kimmeridgian–Berriasian stratigraphy and sedimentary evolution of the central Iberian Rift System (NE Spain)

M. Aurell [a, *], B. Bádenas [a], J.I. Canudo [a], D. Castanera [b], A. García-Penas [a], J.M. Gasca [a], C. Martín-Closas [c], L. Moliner [d], M. Moreno-Azanza [e, f], I. Rosales [g], L. Santas [a], C. Sequero [a], J. Val [a]

[a] Departamento Ciencias de la Tierra-IUCA, Universidad de Zaragoza, 50009, Zaragoza, Spain
[b] Institut Català de Paleontologia Miquel Crusafont, Universitat Autònoma de Barcelona, c/Escola Industrial 23, 08201, Sabadell, Barcelona, Spain
[c] Departament de Dinàmica de la Terra i de l'Oceà, Facultat de Ciències de la Terra, 08028, Barcelona, Spain
[d] Laboratorio ENSAYA, 50410, Cuarte de Huerva, Zaragoza, Spain
[e] Geobiotec, Departamento de Ciências da Terra, Universidade Nova de Lisboa, 2829-526 Caparica, Portugal
[f] GEAL Museu de Lourinhã, Lourinhã, Portugal
[g] Instituto Geológico y Minero de España (IGME), La Calera, 28760, Tres Cantos, Madrid, Spain

ARTICLE INFO

Article history:
Received 12 March 2019
Received in revised form
13 May 2019
Accepted in revised form 30 May 2019
Available online xxx

Keywords:
Tithonian
Berriasian
Iberia
Stratigraphy
Tectono-sedimentary evolution

ABSTRACT

Sequence-stratigraphic, biostratigraphic and strontium-isotopic data have made it possible to update what is known of the stratigraphy and sedimentary evolution of the Kimmeridgian–Berriasian synrift successions recorded in four subbasins (Aguilón, Oliete, Morella, Galve) of the central Iberian Rift System (NE Spain). The studied successions are arranged in three unconformity-bounded synrift sequences. Synrift sequence 1A (Kimmeridgian–mid-early Tithonian) includes four transgressive-regressive sequences deposited on low-angle carbonate ramps, characterized by shallow-water grain-supported facies and coeval open-marine rhythmic successions of marls and lime mudstones (overall thickness ranging from 120 to 250 m). Ammonite biostratigraphy, combined with the last occurrence of *Alveosepta jaccardi* (Schrodt) and strontium-isotopic data constrains the Kimmeridgian-Tithonian boundary towards the uppermost part of synrift sequence 1A. Synrift sequence 1B (mid-early Tithonian to mid-Berriasian) consists of coastal to shallow-marine carbonate to mixed carbonate-siliciclastic successions, with a continuous record in the depocentral areas of the Morella and Galve subbasins (up to 365 m in thickness). *Anchispirocyclina lusitanica* (Egger) is common in the lower and middle part of the sequence, whereas charophytes of the lower Berriasian *Globator maillardii maillardii* Zone are recorded in its upper part. Strontium-isotopic data and ostracods whose first occurrence is Berriasian, indicate that the Tithonian-Berriasian boundary is located towards the mid-upper part of the synrift sequence 1B. Synrift sequence 1C (mid-Berriasian–mid-early Valanginian) is locally recorded in the Galve subbasin and consists of siliciclastic continental successions (up to 100 m in thickness). The available biostratigraphic data (charophytes, ostracods, sporomorphs) indicate that this sequence was deposited upwards from mid-Berriasian *Globator maillardii incrassatus* Zone. The presence of the lower Valanginian successions at the upper part of synrift sequence 1C in certain subsiding areas of the Galve subbasin cannot be ruled out. The sequence-stratigraphic and biostratigraphic data reported here indicate that the Galve and Morella subbasins started to develop around the Kimmeridgian-Tithonian transition. Successive stages of tectonic activity affected these subbasins during the mid-early Tithonian, the mid-Berriasian, and around the Berriasian-Valanginian transition. The stratigraphy and tectono-sedimentary evolution of the central Iberian Rift System indicate that the Berriasian successions are linked to the "Jurassic cycle".

1. Introduction

The problems associated with the definition of the Jurassic-Cretaceous system boundary are largely the result of a lack of significant biostratigraphic markers at the Tithonian-Berriasian and at the Berriasian-Valanginian boundaries, and of faunal provincialism

* Corresponding author.
E-mail address: maurell@unizar.es (M. Aurell).

https://doi.org/10.1016/j.cretres.2019.05.011
0195-6671/

caused by widespread regression (Remane, 1991). Due to this regression, the Tithonian-Berriasian saw major expansion of marginal-marine to continental environments, represented by *Purbeck* and *Weald* facies in many western European basins (e.g., Tennant et al., 2017). In the coeval Tethysian shallow-marine realms, sedimentation on "Jurassic-type" carbonate platforms (predominantly photozoan facies with occasional heterozoan carbonates) ended with the Berriasian, not with the Tithonian (Granier, 2019). Additional difficulties in unravelling the Tithonian–Berriasian sedimentary successions derive from the fact that many of them were deposited coeval to a rifting stage. The analysis and correlation of the continental to shallow-marine successions recorded in active rift basins is generally challenging due to the rapid facies and thickness changes associated with to discontinuous synsedimentary fault activity and subsidence.

The fragmentation of Pangea during the Late Jurassic–Early Cretaceous resulted in intense tectonic activity, on both regional and global scales, with accompanying palaeoceanographic changes including the continued of the opening of the Central Atlantic and Western Tethys (see Tennant et al., 2017 and references therein). The intracratonic Iberian Rift System was part of the network of rifted basins that evolved in the northwestern peri-Tethysian domain (Fig. 1A). Investigations into the southeast Iberian Rift System (i.e., the Maestrazgo Basin) in recent decades have contributed to a progressively increasing understanding of the stratigraphic framework of the Upper Jurassic–Lower Cretaceous synrift successions present in specific key areas at certain time intervals. In particular, the uppermost Jurassic–lowermost Cretaceous marginal-marine to shallow-marine successions of the Maestrazgo Basin have been studied in successive regional works (e.g. Canérot, 1974; Canérot et al., 1982; Salas, 1987; Martín-Closas, 1989; Aurell, 1990; Aurell et al., 1994, 2010, 2016; Salas et al., 2001; Bádenas et al., 2004, 2018; Cobos et al., 2010; Canudo et al., 2012; Campos-Soto et al., 2017, 2019; Liesa et al., 2019). In the western areas of the Maestrazgo Basin, the Tithonian-Berriasian boundary generally occurs within a carbonate to mixed-siliciclastic coastal succession referred to as *Purbeck facies* in pioneer studies (e.g., Canérot, 1974; Meléndez et al., 1979; Gautier, 1980, 1981), or as a *Tithonian–Berriasian Sequence* in later stratigraphic works (e.g., Salas, 1987; Aurell et al., 1994, 2010; Salas et al., 2001; Mas et al., 2004). In these regional studies, the Berriasian successions are traditionally included in the "Jurassic cycle", but the exact location of the Tithonian-Berriasian boundary cannot be established. However, recent reinterpretations based on larger benthic foraminifera biostratigraphy propose an older age for the sedimentation of this succession (mid-Kimmeridgian–Tithonian), questioning the presence of the Berriasian across the western Maestrazgo Basin (Campos-Soto et al., 2019).

The objective of the present work is to integrate the existing information with new sequence-stratigraphic, biostratigraphic (ammonites, benthic foraminifera, charophytes, ostracods) and strontium-isotopic data, providing a more precise account of the chronostratigraphic distribution of the sedimentary successions deposited during the Kimmeridgian–Berriasian in the central part of the Iberian Rift System. The facies distribution and sedimentary evolution documented here reflect the extensional tectonic activity affecting eastern Iberia during this time interval. In particular, the influence on the sedimentation and the nature of the unconformities that developed during successive stages of tectonic activity during the mid-early Tithonian, the mid-Berriasian and around the Berriasian-Valanginian transition have been further documented. Moreover, the reported data provide information about the location of the boundaries of both Tithonian and Berriasian stages within the shallow-marine, coastal to continental Iberian successions.

2. Geological setting

The Late Jurassic–Early Cretaceous rifting event affecting Iberia coincided with the rift propagation from the Central Atlantic northwards and with the opening of the Western Tethys (Salas et al., 2001). The Maestrazgo Basin of eastern Iberia was developed during this rifting event (Fig. 1A). This basin was divided into a set of well-differentiated depocentres (or subbasins) controlled by the synsedimentary activity of local normal faults, which were reactivated or formed during the Late Jurassic–Early Cretaceous rifting (Fig. 1B). The present stratigraphic work concerns the Kimmeridgian–Berriasian synrift successions recorded in four subbasins located in the western part of the Maestrazgo Basin: Aguilón, Oliete, Galve and Morella (Fig. 2A). The northern Aguilón and Oliete subbasins only recorded the Kimmeridgian succession, whereas the Morella and Galve subbasins include a more complete Tithonian–Berriasian succession (Fig. 2B).

The Upper Jurassic-Lower Cretaceous (Kimmeridgian–lower Albian) synrift successions recorded in the studied subbasins have been divided into two synrift sequences, separated by a major synrift unconformity associated with a wide erosional/non-depositional stratigraphic gap of variable amplitude around the Berriasian-Valanginian transition. The interpretation of Liesa et al. (2019) used here (Fig. 2B), updates previous interpretations in which this major synrift unconformity was considered older (i.e. mid-Berriasian: Liesa et al., 1996; Aurell et al., 2016). The lower synrift sequence 1 includes three tectono-sedimentary stages bounded by major unconformities (1A, 1B and 1C in Fig. 2B), with significant changes in the sedimentary systems that developed: (1A) open to shallow-marine Kimmeridgian–lowermost Tithonian carbonate-dominated ramps (e.g. Bádenas and Aurell, 2001; Aurell et al., 2010), (1B) Tithonian–mid-Berriasian coastal to shallow-marine carbonates-siliciclastics (e.g. Aurell et al., 1994), and (1C) locally recorded mid-Berriasian to lowermost Valanginian terrestrial siliciclastics (e.g. Aurell et al., 2016). According to Liesa et al. (2019), synrift sequence 2 also consists of three tectono-sedimentary stages (A, B and C in Fig. 2B) and includes the Valanginian–Barremian continental series or *Weald facies* (Soria et al., 1995; Salas et al., 2001), the uppermost Barremian–Aptian transitional to shallow carbonate platform successions or *Urgonian facies* (e.g. Bover-Arnal et al., 2010), and the lower Albian coal-rich succession of the Escucha Formation (e.g. Querol et al., 1992; Bover-Arnal et al., 2016).

3. Methods

The stratigraphic synthesis presented here is based on published and new data acquired from 36 key reference sections (Fig. 2A and Supplementary data S1), complemented with an extensive review of the available data on the Kimmeridgian–Berriasian successions in other areas of the central Iberian Rift System. In particular, the method of sequence stratigraphy (e.g. Catuneanu et al., 2011) was used in the study area to correlate facies and unconformity-bounded units at different scales, from high-frequency sequences to long-term transgressive-regressive sequences (e.g. Bádenas et al., 2003, 2004; Aurell et al., 2003, 2010; Bádenas and Aurell, 2018; Val et al., 2019). The results reported in these previous works are reviewed and summarized here.

Key intervals of some stratigraphic sections were sampled for strontium-isotopic analysis. Oyster, brachiopod and belemnite shells were collected. The $^{87}Sr/^{86}Sr$ isotopes were determined with a TIMS-Phoenix thermal ionization mass spectrometer at the *CAI Geocronología y Geoquímica Isotópica* of the Universidad Complutense de Madrid (Spain). All $^{87}Sr/^{86}Sr$ data were corrected for possible ^{87}Rb interferences and were normalised to a value of

Please cite this article as: Aurell, M et al., Kimmeridgian–Berriasian stratigraphy and sedimentary evolution of the central Iberian Rift System (NE Spain), Cretaceous Research, https://doi.org/10.1016/j.cretres.2019.05.011

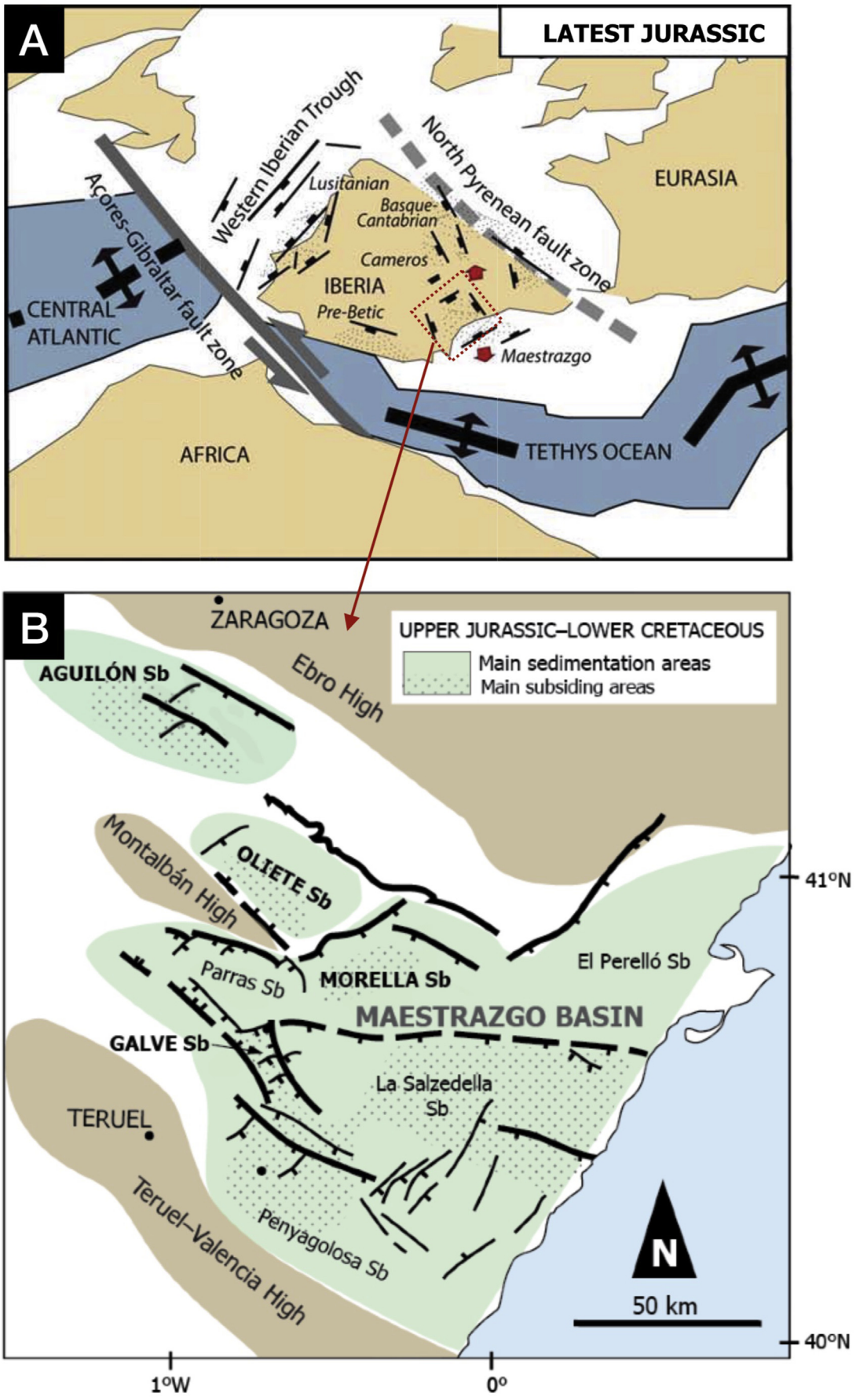

Please cite this article as: Aurell, M et al., Kimmeridgian–Berriasian stratigraphy and sedimentary evolution of the central Iberian Rift System (NE Spain), Cretaceous Research, https://doi.org/10.1016/j.cretres.2019.05.011

0.1194 for $^{87}Sr/^{86}Sr$ in order to correct possible mass-fractionation. During the period of analysis, the NBS-987 standard gave an average $^{87}Sr/^{86}Sr$ value of 0.710246 ± 0.000014 (2σ, n = 9), which was used to correct the measured values from a possible deviation referred to the standard. The analytical error of the $^{87}Sr/^{86}Sr$ ratio referred to 2σ was 0.01%. The comparison between the obtained $^{87}Sr/^{86}Sr$ curve and the global marine $^{87}Sr/^{86}Sr$ curve defined for the Kimmeridgian–Berriasian (McArthur et al., 2012; Wierzbowski et al., 2017), together with biostratigraphical data have allowed a more precise age calibration of the studied units.

For micropaleontological analysis (i.e. ostracods, charophytes), surface bulk samples (1–3 kg) from promising lithologies (marly to mudstone levels) were taken from several sections of the ostracod/charophyte bearing units (i.e. Ladruñán Mb, Aguilar del Alfambra Fm, Galve Fm) in the Morella and Galve subbasins. Processing followed standard methods, treating the samples with water and 2% hydrogen peroxide. The samples were then washed through sieves (1000, 500 and eventually 125 μm mesh) and picked out under a binocular microscope. Selected specimens were scanned with a scanning electron microscope at the University of Zaragoza (JEOL 6400 SEM) and the University of Barcelona. Fossil specimens are housed in the Natural Science Museum of the University of Zaragoza, Spain (Museo de Ciencias Naturales de la Universidad de Zaragoza, MPZ).

4. Stratigraphy

The synthesis of the chronostratigraphic distribution and the correlation of the Kimmeridgian–lowermost Valanginian lithostratigraphic units across the four subbasins under study are shown in Fig. 3. The proposed correlation is the best-fit of the available biostratigraphic, isotopic and sequence-stratigraphic data and in many aspects updates previous stratigraphic interpretations.

The lower datum is the widespread discontinuity (D1) separating the prerift and synrift sequences (Fig. 2B). The age of this discontinuity is well constrained by ammonites in the middle part of the earliest Kimmeridgian *Subnebrodites planula* Zone, at the boundary between the *planula* and *galar* subzones (e.g. Salas et al., 2001; Aurell et al., 2003). In most of the central and eastern Iberian basins, the prerift sequence ends with a middle-upper Oxfordian 10–30 m thick succession of open-platform limestones and marls rich in siliceous sponges and ammonites, which laterally grades into shallow-marine carbonate-siliciclastic successions (e.g. Strasser et al., 2005; Ramajo and Aurell, 2008). The upper datum is the regional intra-rift unconformity (D4) located around the Berriasian-Valanginian transition on the basis of charophytes and foraminifers (e.g. Salas and Casas, 1993, 2001; Martín-Closas and Salas, 1994; Liesa et al., 2019), which corresponds to the boundary between the synrift sequences 1 and 2 (Figs. 2B and 3).

4.1. Aguilón subbasin

The Kimmeridgian successions recorded in the Aguilón subbasin show marked differences between the Ricla and Aguilón sectors (RI and AG: Fig. 3). The Upper Jurassic outcrops located north of the village of Ricla display a continuous exposure of the Kimmeridgian Ki1 and Ki2 sequences (Fig. 4A; Bádenas et al., 2005). These two sequences have a long-term transgressive-regressive facies evolution and are bounded by sedimentary discontinuities that can be traced at basin scale (e.g. Bádenas and Aurell, 2001; Aurell et al., 2010). In Ricla, the lower and middle part of the Ki1 sequence is represented by outer-ramp, marl-dominated successions (upper Sot de Chera Fm, c. 55 m thick) grading upwards to the middle-ramp, burrowed sandy limestones of the lower Loriguilla Fm (c. 60 m thick). The lower and middle part of the upper Sot de Chera Fm includes the ammonites *Sutneria galar* (Oppel) and *Orthosphinctes gigantoplex* (Quenstedt), and the boundary between the *planula* and *platynota* zones is assumed to be located towards the upper part of the Sot de Chera Fm (e.g. Colombié et al., 2014). The upper regressive stage of the Ki1 sequence corresponds to prograding shallow-platform deposits represented by the up to 30 m thick wedge-shaped oolitic-siliciclastic Ricla Mb (Bádenas et al., 2005; Kleipool et al., 2015). The Ricla Mb is bounded on top by a sharp sedimentary discontinuity that represents the Ki1-Ki2 sequence boundary. *Crussoliceras* sp. (early Kimmeridgian, *divisum* Zone) occurs c. 10 m below the Ricla Mb, and the boundary between the Ki1 and Ki2 sequences is assumed to be located near the early-late Kimmeridgian boundary (Val et al., 2017). Q1.2

The thickness of the Ki2 sequence in Ricla ranges from 50 to 60 m. The sequence starts with a condensed limestone level rich in oncoids and skeletal grains, which has been related to a basinwide deepening event (Bádenas and Aurell, 2001). A new strontium-isotopic datum ($^{87}Sr/^{86}Sr$ = 0.706964) from an oyster shell found in this condensed level is coherent with the occurrence of this flooding event at the onset of the late Kimmeridgian (Fig. 5). This condensed level is overlain by middle-ramp reefal limestones that grade distally into a lime mudstone succession (Torrecilla and upper Loriguilla formations, respectively; Bádenas et al., 2005). The skeletal levels found at the top of the Torrecilla Fm contain the benthic foraminifer *Alveosepta jaccardi* (Schrodt). This marine Kimmeridgian succession is overlain by upper Valanginian–Hauterivian continental clastics and carbonates (Soria et al., 1995; Fig. 2B).

The Kimmeridgian rocks form wide outcrops around the AG sector. There, the Ki1 and Ki2 sequences consist of outer ramp marls (Sot de Chera Fm) and lime mudstones (Loriguilla Fm), whereas the Ki3 sequence corresponds to the shallow-ramp carbonates of the Higueruelas Fm (Fig. 4B; Bádenas et al., 2003, 2005; Aurell et al., 2010; Sequero et al., 2018). The age of these sequences is constrained by ammonites, foraminifera and newly acquired strontium-isotopic data (Fig. 3, AG log).

The Ki1 sequence is formed by the marls of the Sot de Chera Fm (c. 50 m thick), including ammonites of the *galar* Subzone (Pérez-Urresti et al., 1998), and by the rhythmic alternation of silty lime mudstones and marls of the lower Loriguilla Fm (40–50 m thick) with scarce early Kimmeridgian ammonites (*Ataxioceratinae*). The Ki2 sequence is formed by up to 60 m of well-bedded lime mudstones of the upper Loriguilla Fm. Significant late Kimmeridgian ammonites found in this unit are *Progeronia breviceps* (Quenstedt) and *Aspidoceras longispinum apeninicum* (Sowerby). *Alveosepta jaccardi* is common in the uppermost part of the Loriguilla Fm (Bádenas et al., 2003).

The Ki3 sequence corresponds to the 50–80 m thick shallow-marine grain-supported peloidal, oncolitic and skeletal limestones of the Higueruelas Fm (see Supplementary data S2). The Higueruelas Fm was assigned in previous work to the lower Tithonian (Aurell, 1990; Ipas et al., 2007; Aurell et al., 2010). However, the record of *Alveosepta jaccardi* and *Redmondelllina powersi* (Redmond) in the uppermost levels of this unit (Fig. 6A and Supplementary data S2), combined with the ammonites found in the underlying Ki2 sequence, indicate that the Ki3 sequence (Higueruelas Fm) in the Aguilón sector was deposited during the late Kimmeridgian, most probably within the late *eudoxus* and *beckeri* zones. The strontium-isotopic ($^{87}Sr/^{86}Sr$) data obtained

Fig. 1. Geological setting: (A) Location of Iberia in the Western Tethys in the latest Jurassic (modified from Liesa et al., 2019); (B) Location of the four studied subbasins, the Aguilón, Oliete, Morella and Galve, within the Maestrazgo Basin.

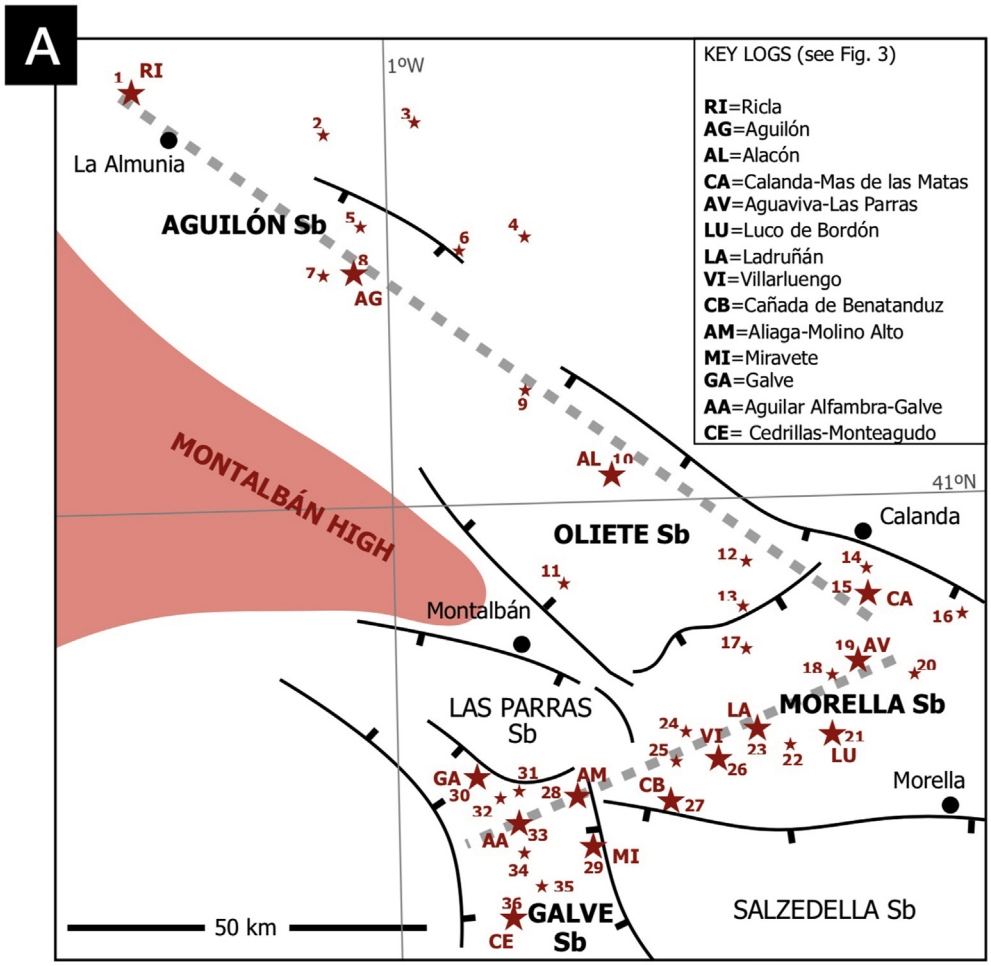

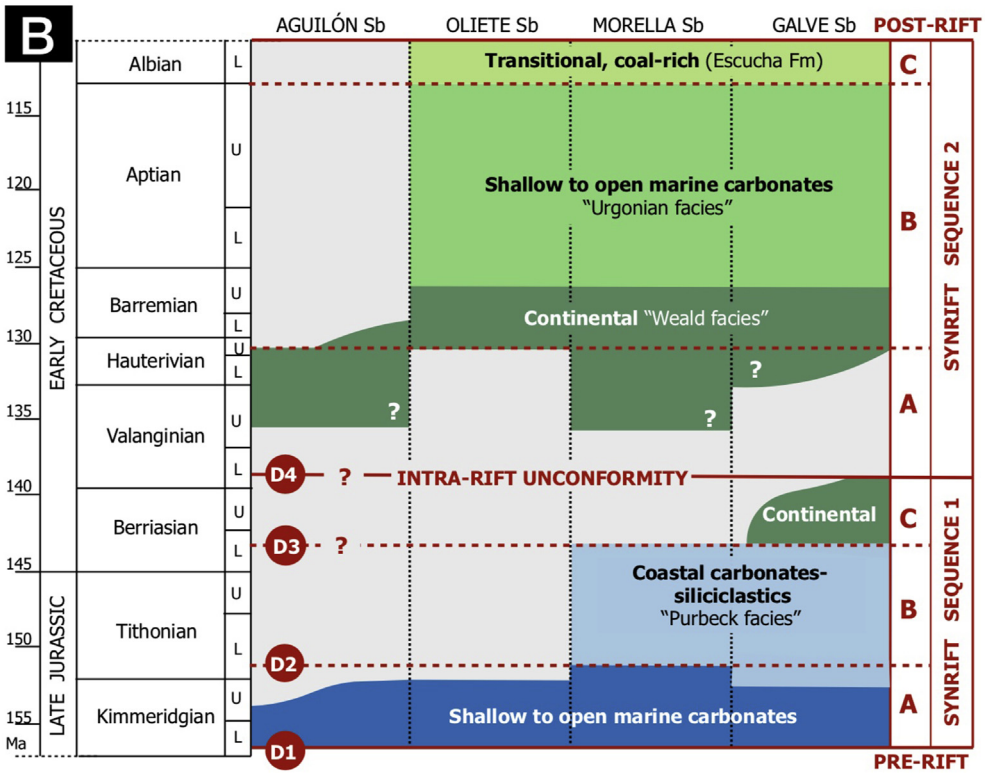

Please cite this article as: Aurell, M et al., Kimmeridgian–Berriasian stratigraphy and sedimentary evolution of the central Iberian Rift System (NE Spain), Cretaceous Research, https://doi.org/10.1016/j.cretres.2019.05.011

from some intervals of the logs of Puebla de Albortón, Fuendetodos and Tosos (logs 4, 6 and 7 in Fig. 2B; see Supplementary data S2) fit well with the global curve of Wierzbowski et al. (2017) during this late Kimmeridgian time interval (Fig. 5). In the area around Aguilón, the upper part of the Ki3 sequence locally consists of an up to 40–70 m thick siliciclastic succession with scarce intercalations of skeletal-rich carbonate beds (Ipas et al., 2007). The skeletal-rich beds found in the lower and middle parts of this siliciclastic-dominated succession still include the Kimmeridgian benthic foraminifera *A. jaccardi* and *R. powersi*. The upper boundary of the Ki3 sequence is an angular unconformity overlain by upper Valanginian–Hauterivian continental facies (Soria et al., 1995; Fig. 2B).

4.2. Oliete subbasin

The Oliete subbasin has an incomplete record of synrift sequence 1A (Fig. 3). During most of the Kimmeridgian, the southwestern area of this subbasin located near the Montalbán High was the deposition site of shallow-marine oolitic and reefal facies (Obón-Torre de las Arcas sector, number 11 in Fig. 2A; Aurell et al., 1999a). Towards the end of the Kimmeridgian, the southern area of the subbasin was eventually exposed and shallow-marine sedimentation became restricted to the north, around the locality of Alacón (AL) (Aurell et al., 2018).

In the more complete Kimmeridgian succession exposed around Alacón (AL log in Fig. 3), synrift sequence 1A includes the Ki1, Ki2 and Ki3 sequences that correspond to the Sot de Chera, Loriguilla, and Higueruelas formations. The Ki1 sequence is formed by the lower Kimmeridgian (*galar* Subzone) marls of the Sot de Chera Fm (up to 20 m thick) and the well-bedded lime mudstones and marls of the lower part of the Loriguilla Fm (c. 40 m). The latter is particularly rich in ammonites, allowing the *platynota* and *hypselocyclum/lothari* early Kimmeridgian ammonite zones to be identified (Moliner, 2009). The Ki2 sequence is represented by the shallow-ramp, grain-supported (peloidal, skeletal) limestones of the Alacón Mb (20–30 m thick). The lower part of this unit includes scarce ammonites from the early part of the late Kimmeridgian (Meléndez et al., 1990). The development of the shallow facies of the Alacón Mb was related to the influence of the Montalbán High (Cepriá et al., 2002). On top of this unit there is a level of pedogenic carbonate breccias developed during the subaerial exposure of the platform after the regional relative seal-level fall associated to the boundary between the Ki2 and Ki3 sequences (Fig. 4C; Aurell et al., 2010). The Ki3 sequence corresponds to the uppermost Kimmeridgian shallow-marine limestones of the Higueruelas Fm (up to 70 m thick). A major erosive unconformity and the associated stratigraphic gap are located above these shallow-marine Kimmeridgian rocks, which are directly overlain by the lower Barremian continental facies that characterizes the onset of the synrift sequence 2 sedimentation in the Oliete subbasin (Aurell et al., 2018; Fig. 2B).

4.3. Morella subbasin

The Kimmeridgian–Berriasian stratigraphy of the Morella subbasin shows marked differences with respect to the coeval sedimentary record in the northwestern Aguilón and the Oliete subbasins. In particular, the lower synrift sequence 1A has a complete record (up to the mid-early Tithonian) in the Morella subbasin, and the synrift sequence 1B is well developed in its depocentral areas (Fig. 3). In most of the northern and central area of the Morella subbasin studied here, the Berriasian successions are unconformably overlain by continental upper Valanginian–Hauterivian lacustrine limestones (Herbers Fm) or equivalent terrigenous continental units (e.g. Canérot, 1974; Gasca et al., 2017; Figs. 2D and 4D).

Synrift sequence 1A starts with the Ki1 sequence, which includes the marls of the Sot de Chera Fm (*galar* Subzone, up to 5 m thick across the whole subbasin) and a 10–30 m thick succession of limestones and marls (Calanda Mb), with a rich-ammonite record of the early Kimmeridgian *platynota*, *hypselocyclum/lothari,* and *divisum* zones (Geyer and Pelleduhn, 1979; Atrops and Meléndez, 1984; Fezer and Geyer, 1988; Meléndez et al., 1990; Finkel, 1992; Moliner, 2009). A prominent discontinuity (hardground) surface located on top of the condensed upper *divisum* Zone marks the boundary between the Ki1 and Ki2 sequences. The upper Kimmeridgian Ki2 and Ki3 sequences are generally represented by a continuous, 60–120 m thick succession of well-bedded, open-marine lime mudstones (Loriguilla Fm). In the outcrops located south of Calanda (CA log in Fig. 3), the upper Loriguilla Fm includes abundant siliceous sponges and ammonites of the *acanthicum*, *eudoxus* and *beckeri* zones (e.g. Geyer and Pelleduhn, 1979). In the Calanda-Val de la Piedra log (log 14 in Fig. 2A), the presence of earliest Tithonian (early *hybonotum* Zone) ammonites in the uppermost part of the Loriguilla Fm has been suggested (Atrops and Meléndez, 1984).

In the upper part of synrift sequence 1A, in the Calanda (CA) sector, most of the Ti1 sequence is formed by the shallow-marine limestones of the Higueruelas Fm (Fig. 3). In the Calanda-Mas de la Matas section (log 15 in Fig. 2A), the Higueruelas Fm consists of a 65 m thick succession of skeletal-peloidal-oncolitic grain-supported limestones, which are locally dolomitized (Aurell et al., 1999b).

In the Villarluengo and Cañada de Benatanduz sectors (see VI and CB in Fig. 3), the upper part of the Ki3 sequence and the Ti1 sequence are represented by thick-bedded limestones with grain-supported oncolitic-peloidal-skeletal facies typical of the Higueruelas Fm. The Kimmeridgian age of the lowermost part of the Higueruelas Fm is indicated by the presence of *Alveosepta jaccardi* in the CB log (log 27 in Fig. 2A).

Synrift sequence 1B is made up of shallow-marine to peritidal carbonate-dominated successions (partly dolomitic) in the Morella subbasin. These thick successions (200–300 m thick) were reported in previous regional stratigraphic analyses (Canérot, 1974; Salas, 1987; Martín-Closas, 1989; Aurell, 1990; Aurell et al., 2010) but were not logged in detail. The results of the logging performed here in three key localities of Aguaviva-Las Parras (AV), Luco de Bordón (LU) and Ladruñán (LA) are summarized in Fig. 7. Around the AV sector, synrift sequence 1B is represented by a 150–250 m thick succession dominated by peritidal, thin-bedded laminated cryptalgal limestones and lime mudstones typical of the La Pleta Fm. Around the LU/LA sector, these peritidal carbonates are located in the lower and upper parts of the sequence, whereas the middle part consists of thick-bedded, mud-to grain-supported shallow-marine carbonates typical of the Bovalar Fm (Fig. 4E). Synrift sequence 1B thus has a long-term transgressive/regressive trend, from the peritidal carbonates of the lower Pleta Fm, to the shallow-marine carbonates of the Bovalar Fm, including levels rich in the benthic foraminifer *Anchispirocyclina lusitanica* (Egger), to the peritidal carbonates of the upper Pleta Fm, and up to the continental to marine-marginal marl-dominated Ladruñán Mb (Fig. 3).

Fig. 2. (A) Distribution of the reference logs (see Supplementary data S1 for names of the logs and key references). The grey dashed line indicates the location of the correlation transect shown in Fig. 3; (B) Synthetic chronostratigraphic distribution of main facies and tectono-sedimentary sequences of the Kimmeridgian–Aptian in the Aguilón, Oliete, Morella and Galve subbasins (adapted from Liesa et al., 2019).

Please cite this article as: Aurell, M et al., Kimmeridgian–Berriasian stratigraphy and sedimentary evolution of the central Iberian Rift System (NE Spain), Cretaceous Research, https://doi.org/10.1016/j.cretres.2019.05.011

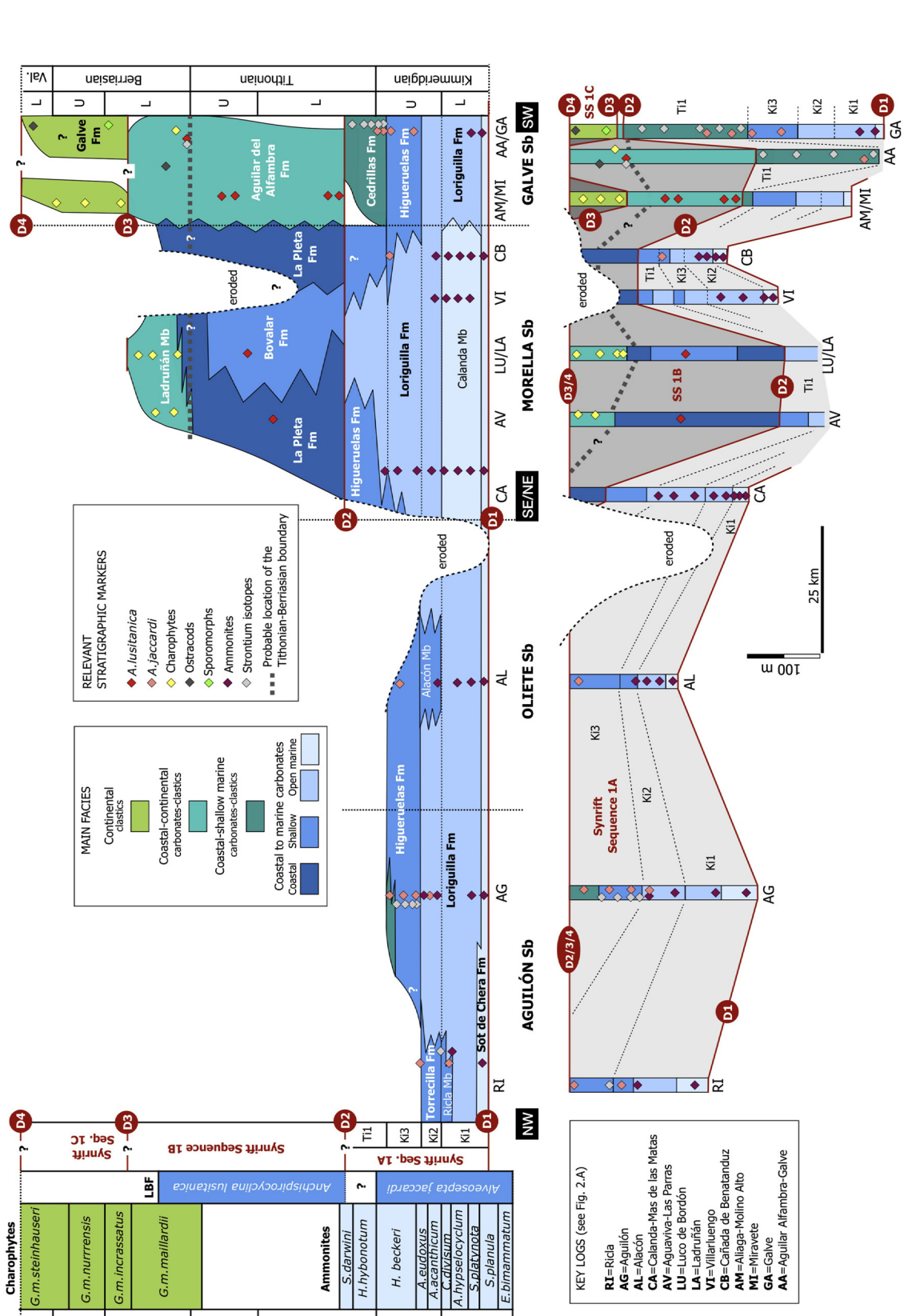

Fig. 3. Chronostratigraphic distribution of lithostratigraphic units of the Kimmeridgian–Berriasian of the Aguilón, Oliete, Morella and Galve subbasins. The lower part shows the thickness of lithostratigraphic units and the location of the relevant stratigraphic markers in the key logs (see Fig. 2A for location). In the upper part, the location of these stratigraphic markers within the unit is based in the assumption of constant average rates of sedimentation. The probable location of the Tithonian-Berriasian boundary in the mid-upper part of synrift sequence (SS) 1B is indicated with a grey dashed-line. The biostratigraphic ranges of the biozones used (ammonites, charophytes, larger benthic foraminifera (LBF)) are shown in the left part. Ammonites are found in the open-marine facies of synrift sequence 1A, foraminifera in the shallow-marine facies of synrift sequences 1A and 1B, and charophytes in the continental to marginal-marine facies of synrift sequences 1B and 1C. Geological Time Scale according to Ogg et al. (2016).

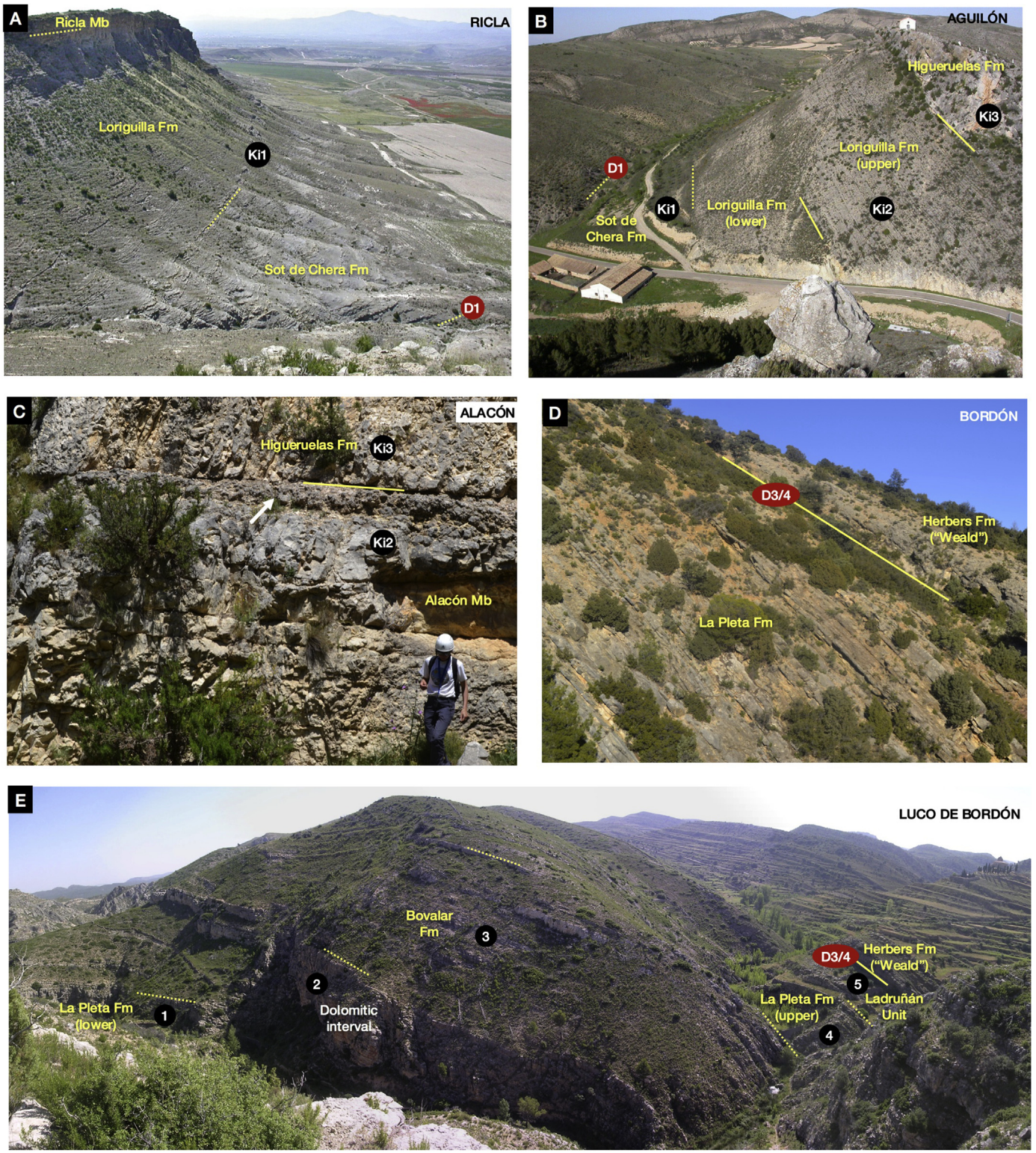

Fig. 4. (A) Distribution of lithostratigraphic units within the Ki1 sequence in Ricla (log 1 in Fig. 2A, Aguilón subbasin); (B) Distribution of lithostratigraphic units within the Ki1, Ki2, and Ki3 sequences in Aguilón (log 8 in Fig. 2A, Aguilón subbasin); (C) Soil development (see white arrow) indicating the subaerial exposure of the platform between the Ki2 and Ki3 sequences in Alacón (log 10 in Fig. 2A, Oliete subbasin); (D) Angular unconformity between the La Pleta Fm (synrift sequence 1B) and the upper Valanginian-Hauterivian lacustrine Herbers Fm in Bordón (log 22 in Fig. 2A, Morella subbasin); (E) Distribution of lithostratigraphic units in Luco de Bordón (log 22 in Fig. 2A). The boundaries of units 1–5 can be traced at regional scale (see Fig. 7).

In these depocentral areas of the Morella subbasin, the synrift sequence 1B consists of five correlatable units (see units 1–5 in Fig. 4E And 7), equivalent to the third-order sequences Ti2-1 to Ti2-5 defined in Aurell et al. (2010). These sequences show a transgressive-regressive or regressive facies evolution and are bounded by widespread sedimentary discontinuities. They display a range and sedimentary evolution comparable to the five third-order sequences 1–5 defined in Bádenas et al. (2004), located

Please cite this article as: Aurell, M et al., Kimmeridgian–Berriasian stratigraphy and sedimentary evolution of the central Iberian Rift System (NE Spain), Cretaceous Research, https://doi.org/10.1016/j.cretres.2019.05.011

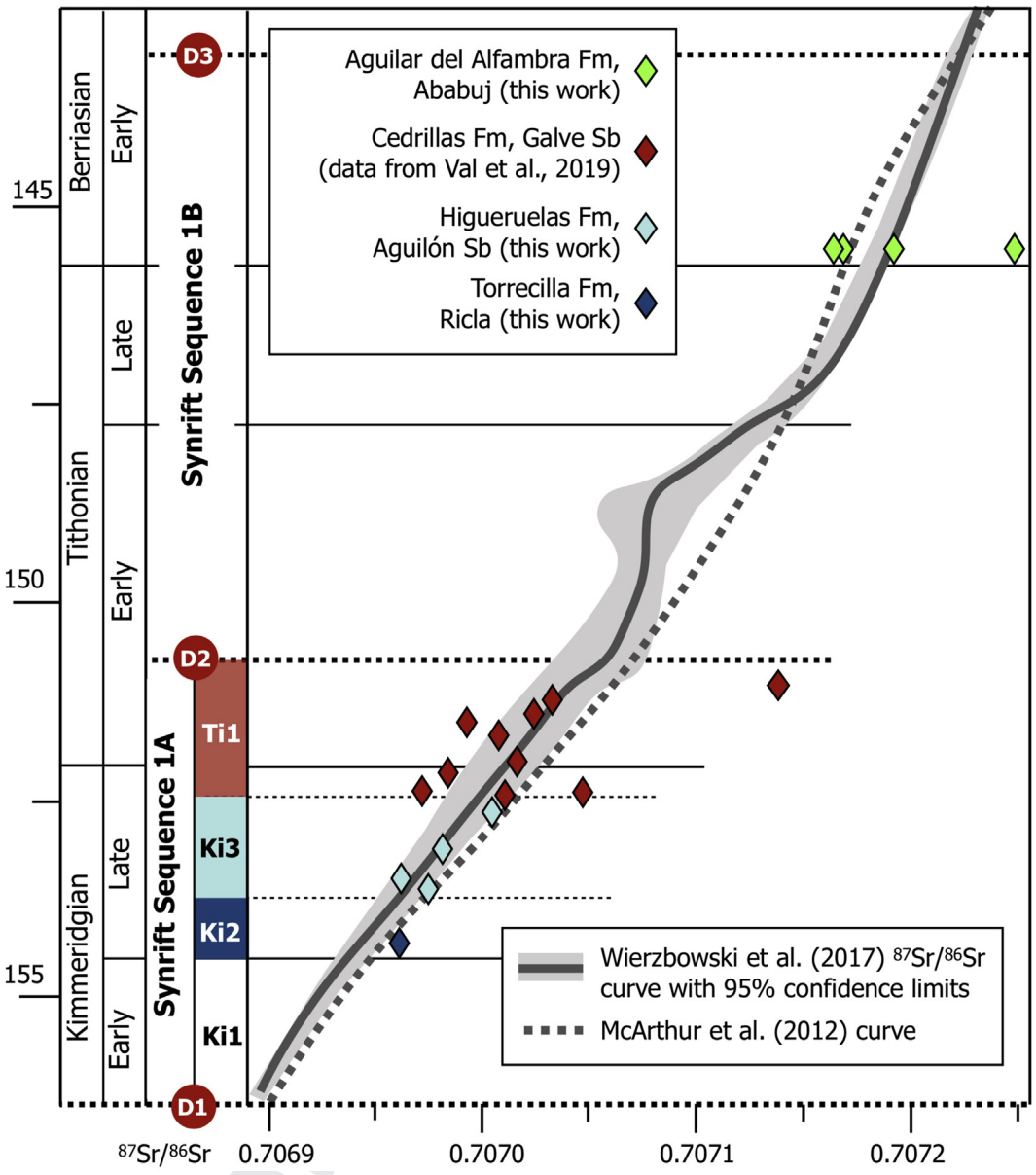

Fig. 5. Strontium-isotopic data ($^{87}Sr/^{86}Sr$) taken from belemnites, brachiopods and oyster shells, and comparison with the global curves of McArthur et al. (2012) and Wierzbowski et al. (2017). For location and data measured in Ricla (sequence Ki2) and Ababuj (synrift sequence 1B) see text. For location and data measured in the Aguilón subbasin (sequence Ki3) see Supplementary data S2. The data from the Galve subbasin (Ti1) were taken from Val et al. (2019). Samples in the Cedrillas and Aguilar del Alfambra formations with abnormally high values are considered as non-reliable and probably reflect a relatively more radiogenic isotopic signal linked to freshwater input (Bryant et al., 1995), in the context of the recorded coastal domains.

further east in the Montanejos and Salzedella sections (i.e. the southern Penyagolosa and Salzedella subbasins, see Fig. 1B).

The Ladruñán Mb includes charophytes of biostratigraphic interest. In particular, analysis of this unit in the localities of Jaganta and Ladruñán (logs 18 and 23 in Fig. 2A) has yielded *Dictyoclavator fieri* (Donze), *Nodosoclavator bradleyi* (Harris), and *Atopochara trivolvis* var. *horrida* (Harris), which characterize the latest Tithonian/mid-early Berriasian *Globator maillardii maillardii* Zone (Canérot, 1974; Martín-Closas, 1989; Riveline et al., 1996). The transition between the La Pleta Fm and the Ladruñán Mb is gradual and is assumed to occur around or above the Tithonian-Berriasian boundary (Fig. 3).

The carbonate successions of synrift sequence 1B are represented around the Cañada de Benatanduz (CB) sector by a 60–90 m thick succession of shallow-marine to thin-bedded peritidal carbonates attributed to the La Pleta Fm. Around the Villarluengo sector, synrift sequence 1B is poorly represented due to the erosion that occurred before the sedimentation of the continental Valanginian–Hauterivian successions (see VI in Fig. 3).

4.4. Galve subbasin

The Galve subbasin shows the most complete record of the studied synrift successions within the study area, because it also includes the local presence of the synrift sequence 1C. In this subbasin, the synrift sequence 1 is overlain by upper Hauterivian–lower Barremian lacustrine to palustrine marls and limestones, which represent the first unit of synrift sequence 2 (Aurell et al., 2016; Fig. 2B).

Please cite this article as: Aurell, M et al., Kimmeridgian–Berriasian stratigraphy and sedimentary evolution of the central Iberian Rift System (NE Spain), Cretaceous Research, https://doi.org/10.1016/j.cretres.2019.05.011

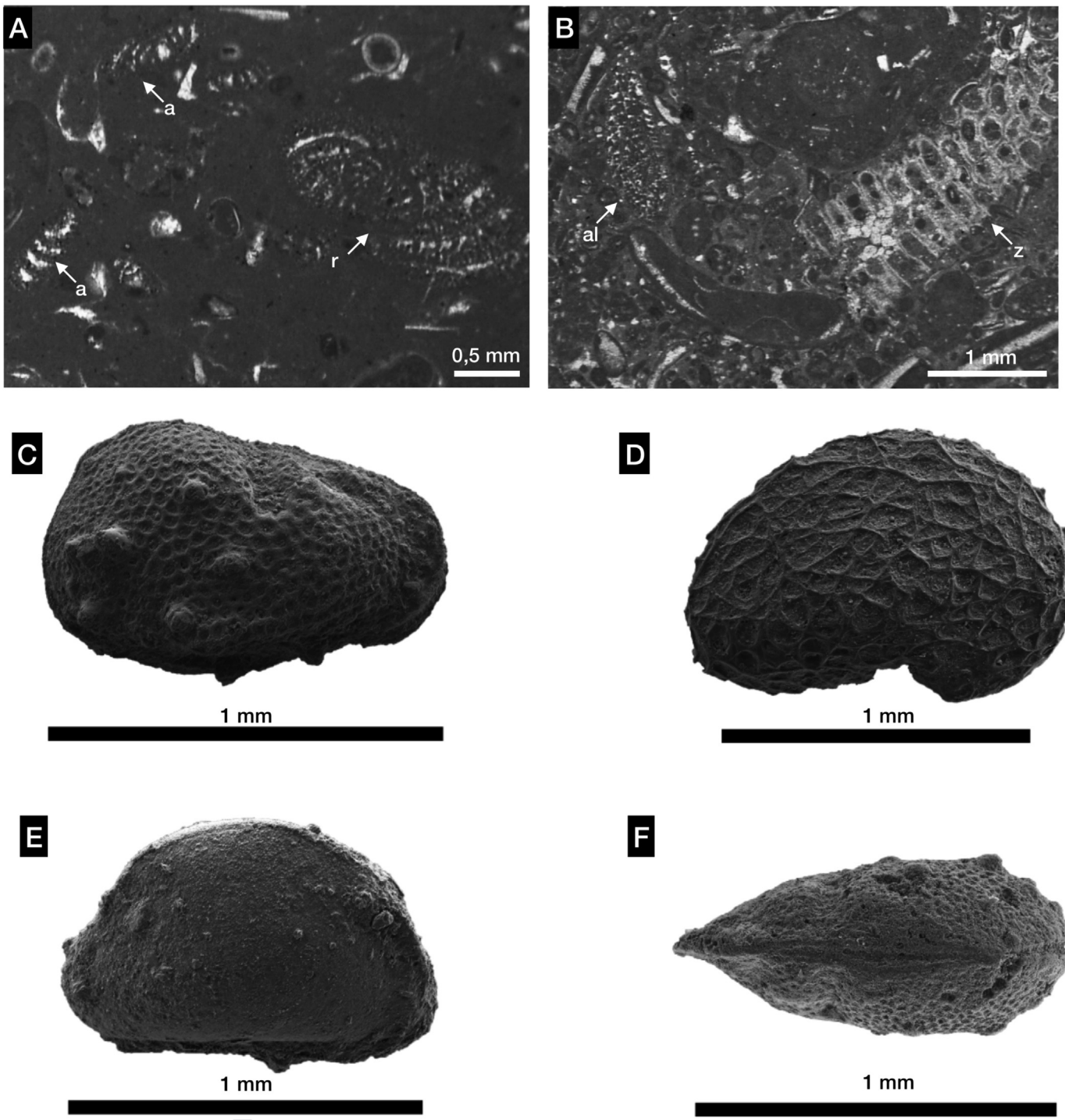

Fig. 6. (A) *Alveosepta jaccardi* (Schrodt) (a) and *Redmondelllina powersi* (Redmond) (r) in skeletal wackestones in the uppermost levels of the Higueruelas Fm (Jaulín log n.3, unit 7, see Supplementary data S2). (B) *Anchispirocyclina lusitanica* (al) and dasycladalean algae *Zergabriella embergeri* (Bouroullec & Deloffre) (z) in peloidal-skeletal packstones of the lowermost levels of the Aguilar del Alfambra Fm (Miravete log n.29, see AM in Fig. 3). (C) MPZ 2019/253, *Theriosynoecum fittoni* (Mantell) from the Aguilar del Alfambra Formation, Cerezos section (log 35; metre 330, Fig. 4 in Aurell et al., 2016); (D) MPZ 2019/254, cf. *Macrodentina* sp. from the Aguilar del Alfambra Formation, Cerezos section (log 35; metre 330, Fig. 4 in Aurell et al., 2016); (E) MPZ 2019/255, cf. *Asciocythere* sp. from the Aguilar del Alfambra Formation, Cerezos section (log 35; metre 330, Fig. 4 in Aurell et al., 2016), (F) MPZ 2019/256, cf. *Theriosynoecum fittoni* from the uppermost part of the Galve Fm in the Galve-Zabacheras log (site 2, Fig. 5 in Aurell et al., 2016).

Synrift sequence 1A has a continuous record across the Galve subbasin, including the Ki1, Ki2, Ki3 a Ti1 sequences. The Ki1 and Ki2 sequences are formed by open-ramp marls and lime mudstones of the Sot de Chera (2–10 m thick) and Loriguilla (90–130 m thick). The lower part of the Loriguilla Fm includes early Kimmeridgian ammonites (Gautier, 1981, Ababuj area), which indicates that the sedimentation of the Loriguilla Fm occurred onwards from the *platynota* Zone. *Alveosepta jaccardi* is present in the Loriguilla Fm and is abundant in the lagoonal skeletal limestones found in the upper part of the overlying Higueruelas Fm. According to the available biostratigraphic and strontium-isotopic data (see Fig. 3), the shallow-marine limestones of the Higueruelas Fm (50–70 m

Please cite this article as: Aurell, M et al., Kimmeridgian–Berriasian stratigraphy and sedimentary evolution of the central Iberian Rift System (NE Spain), Cretaceous Research, https://doi.org/10.1016/j.cretres.2019.05.011

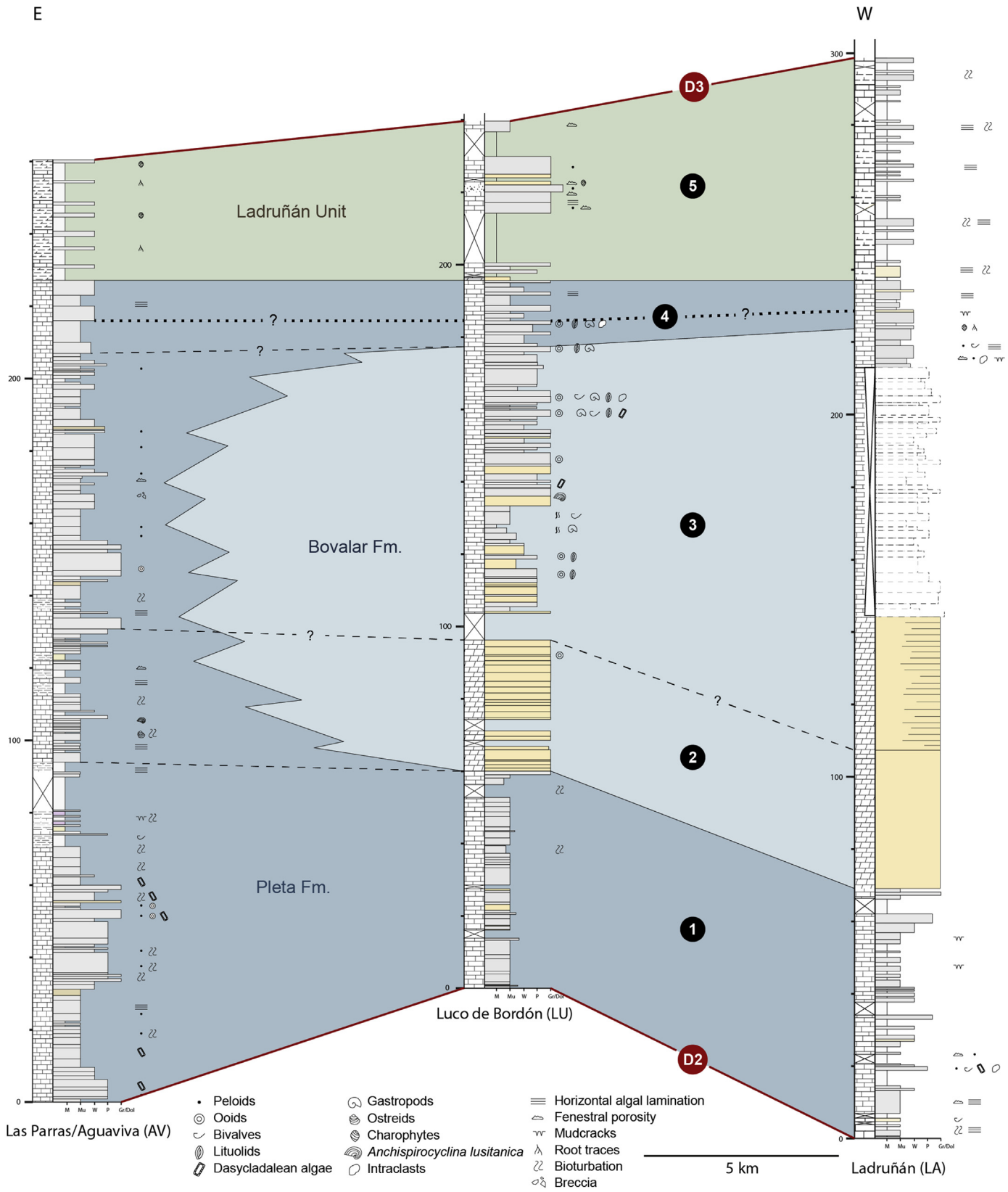

Fig. 7. Correlation of the synrift sequence 1B successions (Tithonian–lower Berriasian) exposed in Las Parras-Aguaviva (AG), Luco de Bordón (LU) and Ladruñán (LA), bounded by major discontinuities D2 and D3. Units 1–5 correspond to the sequences Ti2-1 to Ti2-5 defined in Aurell et al. (2010), which can be traced at regional scale (see Fig. 4E). The Tithonian-Berriasian boundary is probably located in the middle part of unit 4.

Please cite this article as: Aurell, M et al., Kimmeridgian–Berriasian stratigraphy and sedimentary evolution of the central Iberian Rift System (NE Spain), Cretaceous Research, https://doi.org/10.1016/j.cretres.2019.05.011

thick) are interpreted to correspond to the uppermost Kimmeridgian Ki3 sequence. However, Campos-Soto et al. (2019) propose a mid-early Kimmeridgian age for the lower boundary of the Higueruelas Fm (Fig. 8). This interpretation is not consistent with the ammonites found in the underlying open-marine units (i.e. Sot de Chera and Loriguilla formations and Calanda Mb). These open-marine units are younger than the D1 mid-*planula* Zone major discontinuity separating the prerift (Yátova Fm) and synrift sequences (Fig. 2B), and in several localities of the Aguilón, Oliete and Morella subbasins contain late Kimmeridigan ammonites (Fig. 3).

In the Galve subbasin, the onset of the Ti1 sequence is marked by a sharp increase in siliciclastic input. The Ti1 sequence corresponds to the Cedrillas Fm, a new unit formally defined in this work (see Supplementary material S3 for justification and details). The Cedrillas Fm consists of a mixed coastal carbonate-siliciclastic unit well developed in the central and western areas of the subbasin (i.e. Galve, Aguilar del Alfambra, and Cedrillas-Monteagudo; logs 30, 33 and 36 in Fig. 2A). In these areas, this unit ranges from 150 to 220 m in thickness (Fig. 9A). Lower subsidence rates in the eastern marginal areas of the subbasin between Aliaga and Miravete (see AM/MI in Fig. 3) caused a significant reduction in thickness to 10–20 m (Fig. 9B). In the central areas of the Galve subbasin, the Cedrillas Fm consists of four successive sedimentary sequences 30–80 m thick, with a lower interval of well-bedded carbonates (bioclastic, peloidal, ooidal, micritic) and marls, and an upper interval of mudstones including lenticular to tabular cross-bedded sandstones (sequences S1–S4 in Val et al., 2019). The presence of *Alveosepta jaccardi* in the carbonate intervals of the S1 sequence and in the lower part of the S2 sequence (Gautier, 1980; Campos-Soto et al., 2017, 2019; Val et al., 2019), in conjunction with the overall trend of the strontium-isotopic data, indicates a latest Kimmeridgian–mid-early Tithonian age, most probably from the upper part of the *beckeri* Zone up to the transition between the *hybonotum/darwini* zones (Fig. 5; Val et al., 2019). The location of the lower boundary of this unit around the *acanthicum* and *eudoxus* zones proposed by Campos-Soto et al. (2019) is highly speculative and not supported by data (Fig. 8, see boundary between U1 and CLP).

The upper boundary of the Ti1 sequence is a widespread unconformity, which can be traced across the Morella and Galve subbasins (D2 in Fig. 3). Based in the strontium-isotopic data, Val et al. (2019) reassigned the age of this unconformity to the mid-early Tithonian (instead of mid-late Tithonian, in Aurell et al., 2016). In the Galve subbasin, the local presence of a low-angular unconformity associated to this widespread discontinuity indicates block tilting and erosion due to synsedimentary extensional tectonic reactivation at the boundary between synrift sequences 1A and 1B. This erosive surface has been mapped and documented in detail in Galve (García-Penas and Aurell, 2017) and in Aguilar del Alfambra (Aurell et al., 2019).

Synrift sequence 1B corresponds to the Aguilar del Alfambra Fm. This unit varies in thickness across the Galve subbasin (0–365 m) due to strong control by synsedimentary extensional tectonics (Aurell et al., 2016). The Aguilar del Alfambra Fm includes a wide variety of siliciclastic and carbonate facies, which were deposited in a wave-dominated open-coast tidal flat (Bádenas et al., 2018). Similar to what is observed in the Morella subbasin, the synrift sequence 1B has a long-term transgressive/regressive trend, with a transgressive peak indicated by the presence of a bioclastic level (including *Anchispirocyclina lusitanica)* found at the mid-upper part of the unit. This level reached the relatively proximal localities of Aguilar del Alfambra and Ababuj (levels Ag5-2 and Ab5-1 in Bádenas et al., 2018). The biostratigraphic and strontium-isotopic data updated in this work, indicate that the Aguilar del Alfambra Fm spans from the mid-early Tithonian up to the early Berriasian (Fig. 3).

In the Miravete section (log 29 in Fig. 2A), the lowermost part and the middle part of the Aguilar del Alfambra Fm includes *Anchispirocyclina lusitanica* and the dasycladalean algae *Zergabriella embergeri* (Bouroullec & Deloffre) (Fig. 6B). In the Ababuj section (log 34 in Fig. 2A), the bioclastic level Ab5-1 found in the mid-upper part of the unit (metre 245 within the 345 m thick section; see Bádenas et al., 2018) contains the same microfossil association. This level also includes abundant oyster shells that have yielded four stable strontium-isotopic data ($^{87}Sr/^{86}Sr$) of 0.707164, 0.707167, 0.707190 and 0.707249, which, compared with the global curve of Wierzbowski et al. (2017), indicates a latest Tithonian-earliest Berriasian age (Fig. 5).

The presence of scarce ostracods is also relevant in confirming the Berriasian age for the upper part of the Aguilar del Alfambra Fm. *Theriosynoecum fittoni* (Mantell) (Berriasian–Barremian age range; Sames, 2011; Schudack and Schudack, 2012) was found in a fossiliferous level located in the upper part of the unit in the Cerezos section (log 35 in Fig. 2A; level in metre 330 within the 365 m thick section, see Aurell et al., 2016; sequence Ce7 in Bádenas et al., 2018). This level has yielded an additional ostracod assemblage dominated by *T. fittoni* (Fig. 6C) along with scarce specimens of cf. *Macrodentina* sp. (Fig. 6D) and cf. *Asciocythere* sp. (Fig. 6E). The latter taxon, tentatively related to *Asciocythere,* includes species previously described in the La Pleta and El Mangraner formations (*Asciocythere* cf. *circumdata* (Donze)) by Schudack and Schudack (2012). According to these authors (op. cit.), the stratigraphical range of *Asciocythere* cf. *circumdata* is Berriasian whereas other species of *Asciocythere* have also been reported by these authors but not before the Aptian (see Fig. 3 in Schudack and Schudack, 2012). As the geological context allows us to rule out the assignament of the Cerezos section to the Aptian, the presence of *Asciocythere* provides additional evidence of a Berriasian age for the upper part of the Aguilar del Alfambra Formation.

On the other hand, the charophyte specimens found by Canudo et al. (2012) at top of the Aguilar del Alfambra Fm in the Galve-Zabacheras section have been restudied. However, insufficient abundance and poor preservation precluded detailed taxonomic and biostratigraphic attributions. Instead, a new fossil-site located also in the upper part of the Aguilar del Alfambra Fm at La Peñuela outcrop (see location 31 in Fig. 2A) yielded a charophyte assemblage with *Clavator grovesii* var. *grovesii* (Harris) and *Clavator grovesii* var. *discordis* (Shaïkin), which is attributed to the Berriasian, with more probability for the early Berriasian (Martín-Closas, 2000). The location of this new fossil-site is tentatively considered time equivalent to the sequences Ag5 or Ag6 of Bádenas et al. (2018). Campos-Soto et al. (2019) assume that the Aguilar del Alfambra Fm does not reach the Berriasian (see SUP* in Fig. 8). However, the early Berriasian age of the upper part of the unit previously proposed in Aurell et al. (2016) is further confirmed by the new biostratigraphic (carophytes and ostracods) and strontium-isotopic data reported here.

Synrift sequence 1C is represented by the Galve Fm (Fig. 9C). Galve Fm has a discontinuous record and is variable in thicknesses (from 0 to 100 m) across the eastern and western margins of the subbasin. The eastern margin has been studied in detail in the Aliaga-Molino Alto section (log 28-AM, Fig. 2A). There, the Galve Fm consists of red clays with intercalated sandstones and conglomerates representing alluvial fan deposits confined to half-grabens. The recorded charophyte association, with *Atopochara trivolvis horrida* (Harris) and the occasional presence of *Clavator grovesii grovesii* (Harris) and *Atopochara trivolvis micranda* (Grambast), indicates that the sedimentation took place around the early to late Berriasian transition, in the *Globator maillardii incrassatus* and *G.m. nurrensis* zones. The location of the Berrriasian-

Please cite this article as: Aurell, M et al., Kimmeridgian–Berriasian stratigraphy and sedimentary evolution of the central Iberian Rift System (NE Spain), Cretaceous Research, https://doi.org/10.1016/j.cretres.2019.05.011

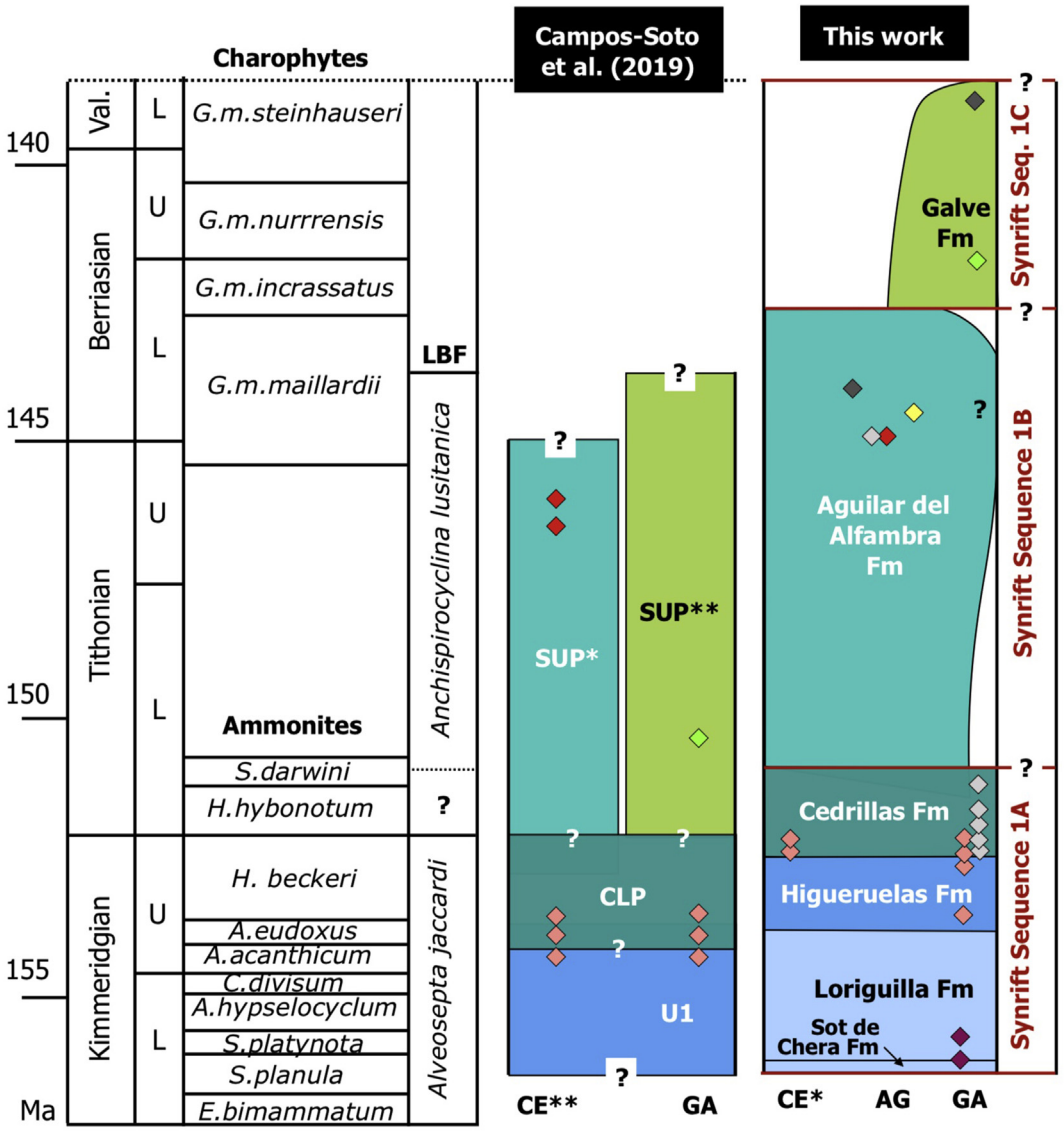

Informal units of Campos-Soto et al. (2019) and correspondence to the **formal lithostratigraphic units** (Aurell et al. 2016, this work)

SUP**= siliciclastic upper part (equivalent to **Galve Fm**)
SUP*= siliciclastic upper part (equivalent to **Aguilar del Alfambra Fm**)
CLP*= carbonate-dominated lower part (equivalent to **Cedrillas Fm**)
U1= see Diaz-Molina and Yébenes (1987) (equivalent to **Higueruelas Fm**)

RELEVANT STRATIGRAPHIC MARKERS

- *A.lusitanica* (Aurell et al., 2016; Campos-Soto et al., 2017)
- *A.jaccardi* (Campos-Soto et al., 2017, 2019; Val et al., 2019)
- Charophytes (La Peñuela, this work)
- Ostracods (Aurell et al., 2016; this work)
- Sporomorphs (Santos et al., 2016)
- Ammonites (Gautier, 1980, 1981)
- Strontium isotopes (Val et al., 2019; this work)

MAIN FACIES
Continental clastics
Marginal to shallow marine carbonates-clastics
Marine carbonates
Shallow Open marine

KEY LOCALITIES
GA=Galve-Zabacheras
AG=Aguilar del Alfambra
CE*=Cedrillas-Monteagudo
CE**=Cedrillas-western Penyagolosa subbasin

Please cite this article as: Aurell, M et al., Kimmeridgian–Berriasian stratigraphy and sedimentary evolution of the central Iberian Rift System (NE Spain), Cretaceous Research, https://doi.org/10.1016/j.cretres.2019.05.011

Valanginian boundary towards the upper part of this succession cannot be rulet out (Aurell et al., 2016; see Fig. 10 therein).

Westwards, around the locality of Galve (log 30-GA, Fig. 2A), the Galve Fm consists of red clays with intercalated cross-bedded and tabular-burrowed sandstones representing channel and overbank deposits in an alluvial floodplain. Santos et al. (2018) report on the sporomorph assemblage in the lower part of the Galve Fm (Las Zabacheras fossil site, Galve-Zabacheras section), indicating the presence of some taxa whose first occurrence is Berriasian (in particular, *Cicatricosisporites imbricatus* (Markova)) and other taxa whose last occurrence has been reported in the lower Valanginian (*Impardecispora canadensis* (Pocock)). Furthermore, in the Galve-Zabacheras section, a marly level located in the upper part of the Galve Fm (see site number 2 in Fig. 5 of Aurell et al., 2016) has yielded numerous specimens of the Berriasian–Barremian ostracod *Theriosynoecum fittoni* (Fig. 6F), as well as an isolated charophyte specimen that was attributed by Canudo et al. (2012) to the latest Berriasian–Hauterivian *Globator maillardii steinhauserii* (Mojon). However, this assignment could not be confirmed in the present review.

In summary, the set of biostratigraphic data summarized above indicates that, in the Galve subbasin, the onset of the sedimentation of the Galve Fm occurred in the mid-Berriasian, around the boundary between the *G. m. maillardii and G. m. incrassatus* zones. In addition, the possible location of the Berriasian-Valanginian boundary towards the upper part of the Galve Fm remains uncertain (Aurell et al., 2016). In contrast, Campos-Soto et al. (2019) propose a Tithonian–mid-early Berriasian age for the Galve Fm in the Galve-Zabacheras outcrop (Fig. 8, see SUP** in GA). However, this age assignment is not consistent with the available biostratigraphic data, in particular by the Berriasian-lower Valanginian sporomorph assemblage found in the lower part of the Galve Fm in the Zabacheras fossil site (Santos et al., 2018). Moreover, these authors regard the mixed carbonate-siliciclastic marginal-marine deposits of the Aguilar del Alfambra Fm time equivalent to the continental siliciclastics of the Galve Fm (see SUP* and SUP** in Fig. 8). However, this interpretation is not consistent with the regional tectono-stratigraphic data, with the presence of an intermediate angular unconformity between these two units, which has been mapped in separated areas of the Galve subbasin (see Aurell et al., 2016 for details, in particular Figs. 6 and 9 therein, and García-Penas and Aurell, 2017).

5. Facies distribution and tectono-sedimentary evolution

The Upper Jurassic carbonate ramps that developed in eastern Iberia had a well-defined distribution of facies belts ranging from proximal (western) to distal (eastern) locations (e.g., Bádenas and Aurell, 2001). Differential tectonics involving the uplift of the marginal (western) areas of the Iberian Rift System from the latest Jurassic on, combined with a long-term regional fall in sea level, resulted in the progressive eastwards coastal offlap of these carbonate ramps (Aurell et al., 1994, 2003). In the subbasins under study, the observed facies evolution from the Kimmeridgian carbonate ramp successions to the Tithonian–Berriasian marginal-marine to continental carbonate to siliciclastic-dominated units allows the progressive eastward shoreline migration to be reconstructed in detail (Fig. 10).

At the onset of the synrift sequence 1A, during the deposition of sequences Ki1 and Ki2, wide carbonate ramps were developed in eastern Iberia. In the studied area, there are no significant lateral changes in thickness in the recorded Kimmeridgian successions (Sot de Chera, Loriguilla, Torrecilla formations and Ricla Mb; Fig. 3), indicating that there was not individualization of different subbasins at the time (Fig. 10A). However, the Montalbán High was already uplifted and influenced the distribution of the shallow (Alacón Mb) to open-marine facies (Loriguilla Fm; Cepriá et al., 2002; Aurell et al., 2018). Southwards of the study area, differential tectonic activity controlled the formation of the Salzedella subbasin (Salas, 1987; Bádenas and Aurell, 2001).

At the end of synrift sequence 1A, during the sedimentation of the Ki3 and Ti1 sequences (Loriguilla, Higueruelas, and Cedrillas formations), significant offlap resulted from the eventual restriction of sedimentation in the easternmost part of the study area (Fig. 10B). The Galve subbasin started to develop around the Kimmeridgian-Tithonian transition. The accommodation created in the central and eastern depocentral areas was filled by the thick coastal siliciclastic-carbonate successions of the Ti1 sequence (Cedrillas Fm; Val et al., 2019).

The Tithonian–early Berriasian synsedimentary tectonics resulted in marked differences between the continental, coastal and shallow-marine successions of synrift sequence 1B recorded in the Galve and Morella subbasins (Fig. 3). The sedimentation consisted mainly of coastal mixed carbonate-siliciclastic-dominated successions in the Galve subbasin (Aguilar del Alfambra Fm; Bádenas et al., 2018), whereas peritidal to shallow-marine carbonates occurred in the newly formed Morella subbasin (La Pleta and Bovalar formations and Ladruñán Mb; Fig. 10C).

During the late Berriasian–mid-early Valanginian, the continental sedimentation of synrift sequence 1C in the study area became restricted to small isolated grabens or half-grabens that developed in the Galve subbasin (Galve Fm; Fig. 10D). The synsedimentary tectonic activity during the sedimentation of this sequence was irregular and discontinuous. Continental to marine-marginal carbonate-dominated sedimentation around the Berriasian-Valanginian transition occurred southeastwards of the study area, in the Salzedella subbasin (Canérot et al., 1982; Martín-Closas and Salas, 1994; Salas et al., 2001; Bádenas et al., 2004).

The tectono-sedimentary evolution of the central Iberian Rift System reconstructed here deepens our understanding of the gradual propagation of synsedimentary tectonics associated with the initial stages of the Late Jurassic–Early Cretaceous rifting (Aurell et al., 1994; Salas et al., 2001). Differential subsidence giving rise to the individualization of the southeastern Salzedella subbasin started during the earliest Kimmeridgian (Salas, 1987; Bádenas and Aurell, 2001). The Galve and Morella subbasins characterized here started to develop later, in the latest Kimmeridigan and the early Tithonian, respectively. Finally, the northwestern Aguilón and Oliete subbasins were developed later still, during the mid-Valanginian and early Barremian stages, respectively (Soria et al., 1995; Aurell et al., 2018).

6. Discussion

The combination of biostratigraphic (ammonite and microfossil assemblages), sequence-stratigraphic and strontium-isotopic data compiled in this study allows us to constrain the

Fig. 8. Comparison between the Kimmeridgian–Berriasian stratigraphy of the Galve and western Penyagolosa subbasins proposed by Campos-Soto et al. (2019) and in this work. The correspondence between the names of the informal units used in Fig. 3 of Campos-Soto et al. (2019) and the formal lithostratigraphic units used here is indicated in the lower part of the figure. See text for explanation and discussion on the observed discrepancies. The location of the key stratigraphic markers within each unit is based in the assumption of constant average rates of sedimentation (distribution of the benthic foraminifera in the Cedrillas log taken from Campos-Soto et al., 2019).

Please cite this article as: Aurell, M et al., Kimmeridgian–Berriasian stratigraphy and sedimentary evolution of the central Iberian Rift System (NE Spain), Cretaceous Research, https://doi.org/10.1016/j.cretres.2019.05.011

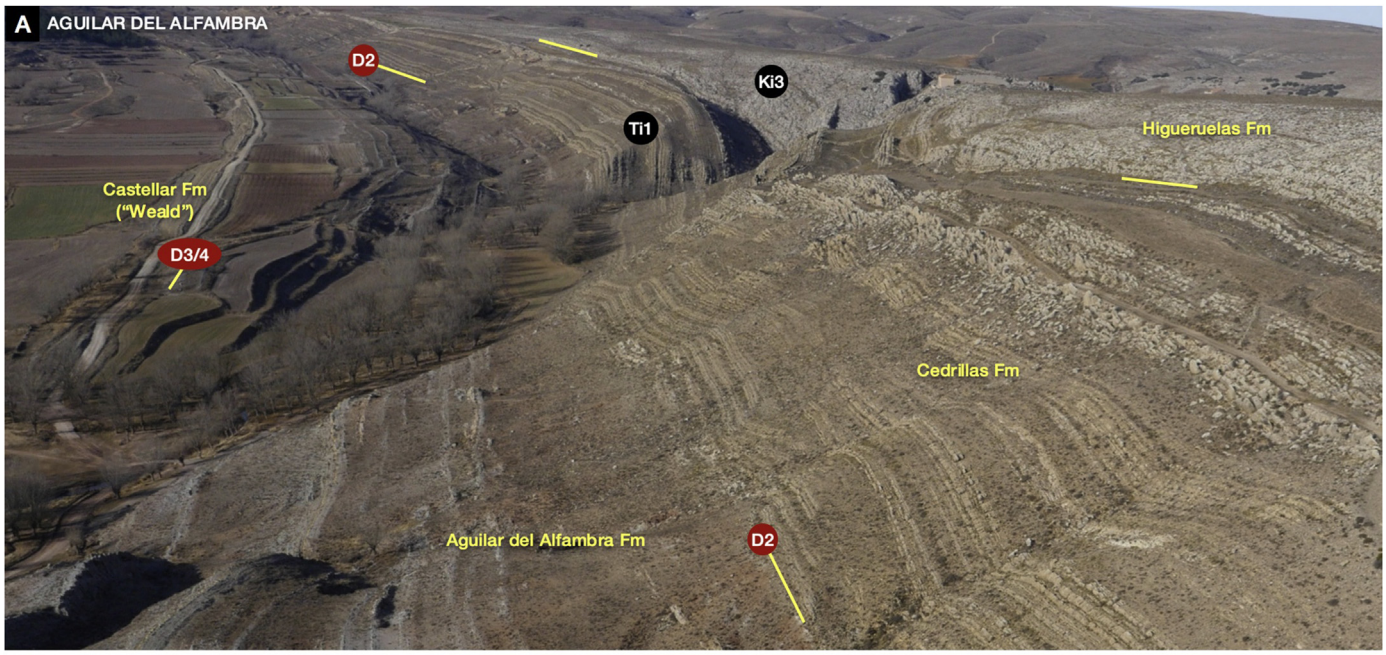

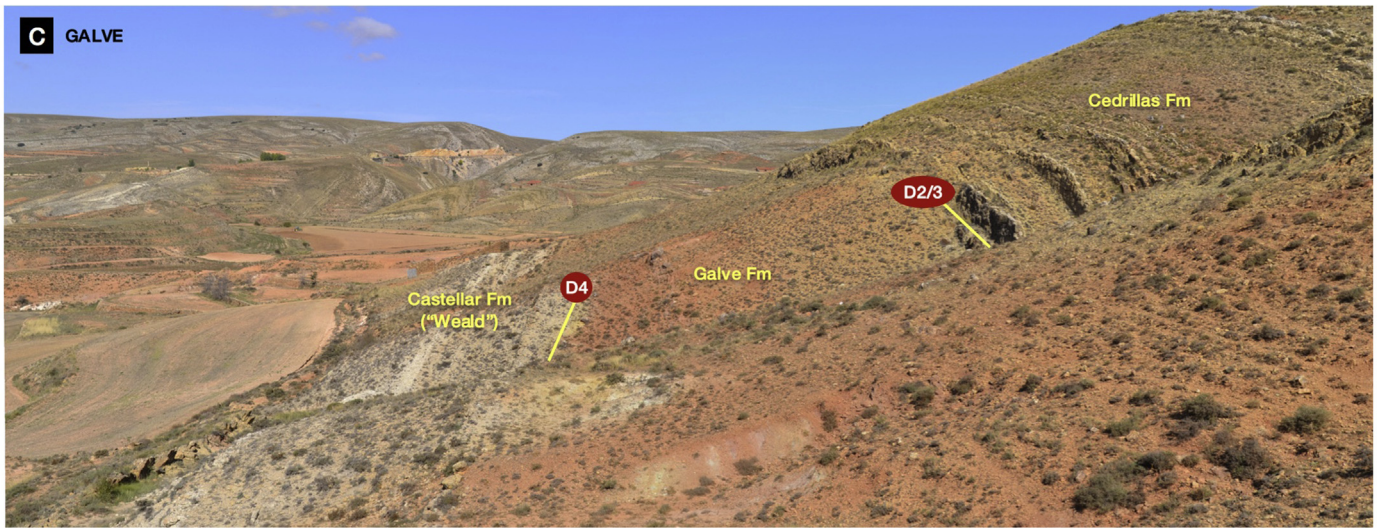

Please cite this article as: Aurell, M et al., Kimmeridgian–Berriasian stratigraphy and sedimentary evolution of the central Iberian Rift System (NE Spain), Cretaceous Research, https://doi.org/10.1016/j.cretres.2019.05.011

chronostratigraphic framework of the Kimmeridgian–lowermost Valanginian (?) sedimentary record in the central part of the Iberian Rift System. In particular, the present work makes it possible to discuss the position of the lower and upper boundaries of the Tithonian and Berriasian stages.

The Kimmeridgian-Tithonian boundary occurs in the uppermost part of the synrift sequence 1A (Fig. 3). The location of this boundary is based on the presence of late Kimmeridgian ammonites in the K2 and Ki3 sequences, the last occurrence of *Alveosepta jaccardi* in the lower part of the Ti1 sequence, and strontium-isotopic data obtained from the Higueruelas Fm (Aguilón subbasin) and Cedrillas Fm (Galve subbasin). Neither *A. jaccardi*, nor *Anchispirocyclina lusitanica* has been found in the middle and upper part of the Ti1 sequence in the Galve and Morella subbasins, despite the existence of shallow-marine to lagoonal carbonate intervals rich in lituolids. However, in some localities in the Galve subbasin (Miravete-MI log, Aguilar del Alfambra Fm; Fig. 3), *A. lusitanica* has been found in the lowermost levels of the overlying synrift sequence 1B. Bádenas et al. (2004) also report on the occurrence of *A. lusitanica* starting from the onset of the time-equivalent Bovalar Fm (Montanejos and Salzedella sections). The available data in eastern Iberia thus lend support to the proposals put forward by Ramalho (1981) for the Lusitanian Basin and Peybernès (1998) for the European basins, according to which the first occurrence of *A. lusitanica* was not at the onset of the Tithonian but rather in the middle part of the early Tithonian, after the *hybonotum*/*darwini* ammonite zones (Fig. 11). The last occurrence of *A. lusitanica* has been reported to reach the mid-early Berriasian (e.g., Ramalho, 1981; Peybernès, 1988; Granier, 2019).

As regards the position of the Tithonian-Berriasian boundary in the studied area, this can be approached with the data available for the mid-upper part of the synrift sequence 1B (see dark grey dashed line in Fig. 3). In the Morella subbasin, this boundary is most probably located close to the boundary between the peritidal carbonates of the La Pleta Fm and the charophyte-rich marly-dominated succession of the Ladruñán Mb. In the Galve subbasin, the strontium-isotopic data and the presence of ostracods whose first occurrence is in the Berriasian indicate that the Tithonian-Berriasian boundary is probably found towards the middle-upper part of the coastal mixed carbonate-siliciclastic succession of the Aguilar del Alfambra Fm.

The Berriasian-Valanginian boundary has been tentatively located at the upper part of synrift sequence 1C (Galve Fm, Fig. 3; see also Aurell et al., 2016). In the Galve subbasin, the largest stratigraphic gap occurs in association with the D4 synrift unconformity (Fig. 2B). For this reason, the D4 unconformity (most probably located at the earliest Valanginian) is here considered to be the boundary between the "Jurassic" and the "Lower Cretaceous" cycles (or synrift sequences 1 and 2; see also Liesa et al., 2019). Eastwards, in the Salzedella subbasin, there is evidence of a continuous sedimentation across the Berriasian–Valanginian boundary. Of particular interest are the continental carbonates of the El Mangraner Fm. In its type locality, the boundary between the *Globator maillardii nurrensis* and *G. m. steinhauseri* charophyte zone is located in the lower part of the El Mangraner Fm, and the age of this unit ranges from late Berriasian to early Valanginian (Salas et al., 1995; Martín-Closas and Salas, 1994, 1998). Northeastwards, in the Garraf Basin, the El Mangraner Fm includes charophytes of the late Berriasian *G. m. nurrensis* Zone (Albrich et al., 2006). In any case, the stratigraphic and tectono-sedimentary evolution of the different subbasins of the Maestrazgo Basin indicates that the Berriasian succession is related to the "Jurassic cycle", not to the "Lower Cretaceous cycle".

Despite the imprint of synsedimentary tectonics, the sequential architecture observed in the Kimmeridgian–early Berriasian Iberian marine successions has been related in previous work to eustatic and/or climatic changes driven by orbital cycles. In particular, the influence of the short and long eccentricity cycles has been found not only in the shallow-to open-marine domains of the Ki2 and Ki3 sequences (e.g., Bádenas et al., 2005; Bádenas and Aurell, 2018), but also in the mixed carbonate-siliciclastic shallow-marine to coastal succession of the Ti1 sequence deposited in the Galve subbasin around the Kimmeridgian-Tithonian transition (Val et al., 2019), and in the mid-Tithonian to earliest Berriasian shallow-marine carbonate-dominated successions that include *Anchispirocyclina lusitanica*, well recorded in the depocentral areas of the eastern part of the Maestrazgo Basin (Salzedella and Montanejos sections, Bovalar Fm: Bádenas et al., 2004). This cyclostratigraphic analysis gives further support to the stratigraphic framework proposed here. The time calibration of the studied Kimmeridgian–Berriasian synrift successions (Fig. 3), is coherent with the overall duration based on the number of high-frequency sequences that previous work have proposed were formed in tune with the short (100 ky) and long (400 ky) eccentricity orbital cycles (Fig. 11). In particular, the upper part of synrift sequence 1A (Ki2, Ki3 and Ti1 sequences) includes 10 sequences formed in tune with the long eccentricity cycle (total duration of c.4 Myr), which fits the 3.7 Myr duration of this time interval proposed here. Moreover, the lower and middle part of the synrift sequence 1B including *Anchispirocyclina lusitanica* of c.7 Myr of duration, fits well with the 57–60 sequences formed in tune with the short-eccentricity cycle in the Bovalar Fm (Fig. 11). It is interesting to note that the influence of the long and short eccentricity cycles during the Kimmeridgian–Berriasian has also been reported from other, distant sedimentary domains (i.e. the Swiss Jura carbonate platform: Strasser, 1988, 2007; Colombié and Strasser, 2005), reinforcing the idea of a global eustatic/climatic signal influencing the sedimentation.

7. Conclusion

The Kimmeridgian–Berriasian synrift successions recorded in the central Iberian Rift System (NE Spain) consist of three synrift sequences (1A, 1B and 1C) bounded by major unconformities. These sequences have an irregular and variable record across the four studied subbasins, the Aguilón, Oliete, Morella, and Galve.

The Kimmeridgian–lowermost Tithonian synrift sequence 1A (150–400 m thick) consists of four transgressive-regressive sequences (Ki1, Ki2, Ki3 and Ti1 sequences). These sequences formed on successive low-angle carbonate ramps, characterized by grain-supported facies in shallow areas (including abundant levels with *Alveosepta jaccardi*), which graded offshore to monotonous successions of marls and lime mudstones, including ammonites that allow the precise biostratigraphic calibration of these successions. The progressive eastern offlap of these carbonate ramps resulted in the reduced extension of the uppermost Kimmeridgian–lower Tithonian Ti1 sequence, which is only recorded in the eastern Morella and the Galve subbasins. Grain-supported carbonates are predominant in the marginal areas of the Morella subbasin, whereas mixed carbonate-siliciclastic coastal sediments developed coevally around the Kimmeridgian-Tithonian transition in the Galve subbasin.

Fig. 9. Representative field views showing the distribution of lithostratigraphic units in the Galve subbasin. (A) Aguilar del Alfambra section (log 33 in Fig. 2A); notice that the Galve Fm is absent; (B) Miravete section (log 29 in Fig. 2A); notice that the Cedrillas Fm is very reduced in thickness; (C) Eastern flank of the Galve syncline (log 30 in Fig. 2A); notice that the Aguilar del Alfambra Fm is absent.

Please cite this article as: Aurell, M et al., Kimmeridgian–Berriasian stratigraphy and sedimentary evolution of the central Iberian Rift System (NE Spain), Cretaceous Research, https://doi.org/10.1016/j.cretres.2019.05.011

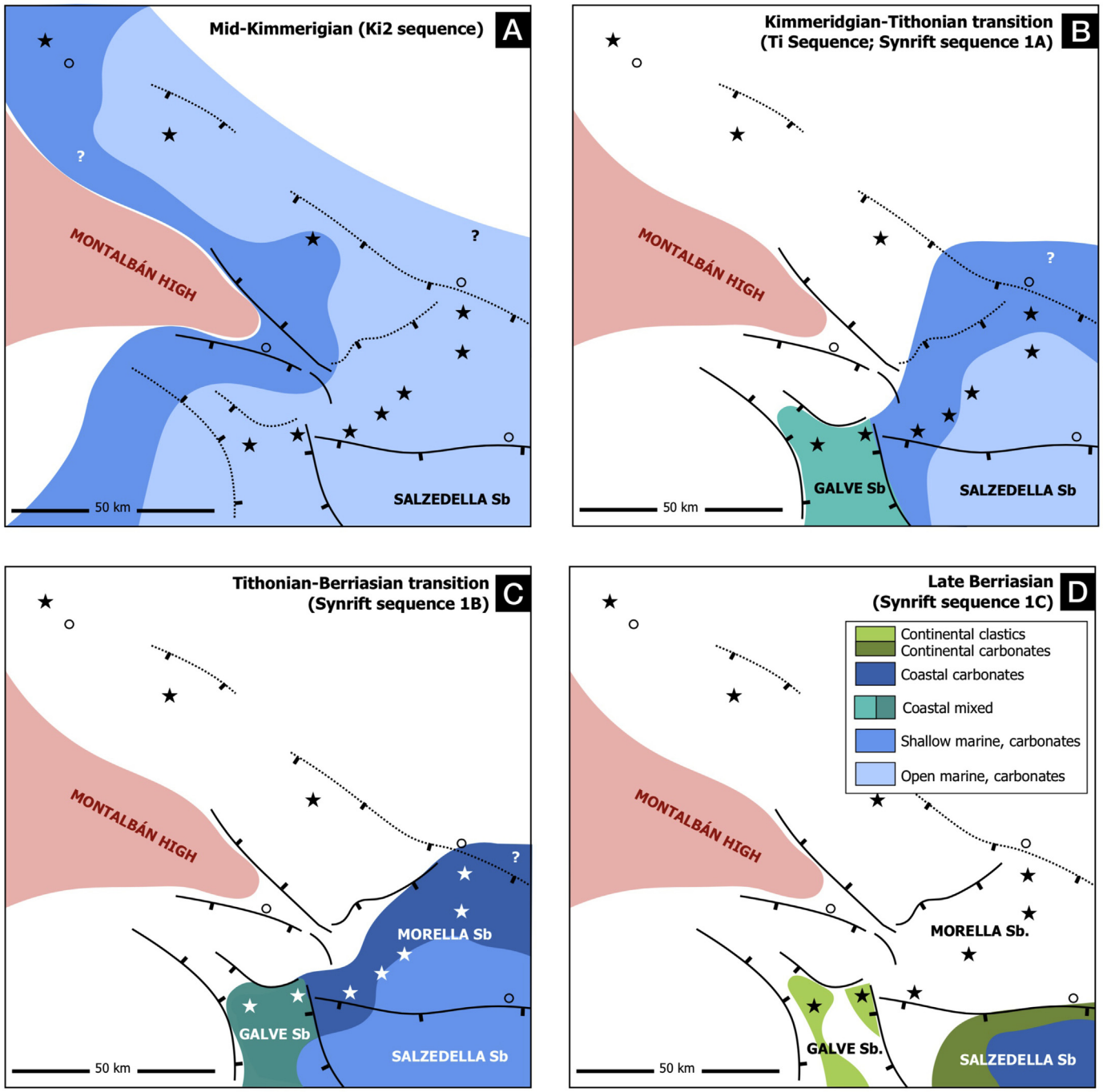

Fig. 10. Paleogeographic evolution of the central Iberian Rift System from mid-Kimmeridgian to late Berriasian. The information in D for the Salzedella subbasin is compiled from Canérot et al. (1982), Salas (1987), and Martín-Closas and Salas (1994).

A major sedimentary change associated with normal fault reactivation occurred at the onset of synrift sequence 1B, during the mid-early Tithonian. Differential subsidence resulted in the local accumulation of a thick (up to 365 m) coastal to shallow-marine carbonate and siliciclastic successions in the depocentral areas of the Morella and Galve subbasins. The age of synrift sequence 1B (mid-early Tithonian to mid-Berriasian) is constrained by the presence of the benthic foraminifera *Anchispirocyclina lusitanica*, strontium-isotopic data, and the occurrence of charophytes of the *Globator maillardii maillardii* Zone in the upper part of the sequence. According to the available data, the Tithonian-Berriasian boundary is located towards the mid-upper part of synrift sequence 1B. In the Morella subbasin, this boundary is likely to be located around the boundary between the La Pleta Fm and the Ladruñan Mb. In the Galve subbasin, the strontium-isotopic data suggest that this boundary is found in the mid-upper part of the Aguilar del Alfambra Fm.

Sedimentation of the mid-Berriasian–lowermost Valanginian synrift sequence 1C was irregular and is only represented in certain areas of the Galve subbasin, which records the up to 100 m thick continental succession of the Galve Fm. Biostratigraphic data constraining the age of the Galve Fm are provided by charophytes, ostracods, and sporomorphs. Sedimentation of this unit occurred during a phase of intense tectonic activity that involved the

Please cite this article as: Aurell, M et al., Kimmeridgian–Berriasian stratigraphy and sedimentary evolution of the central Iberian Rift System (NE Spain), Cretaceous Research, https://doi.org/10.1016/j.cretres.2019.05.011

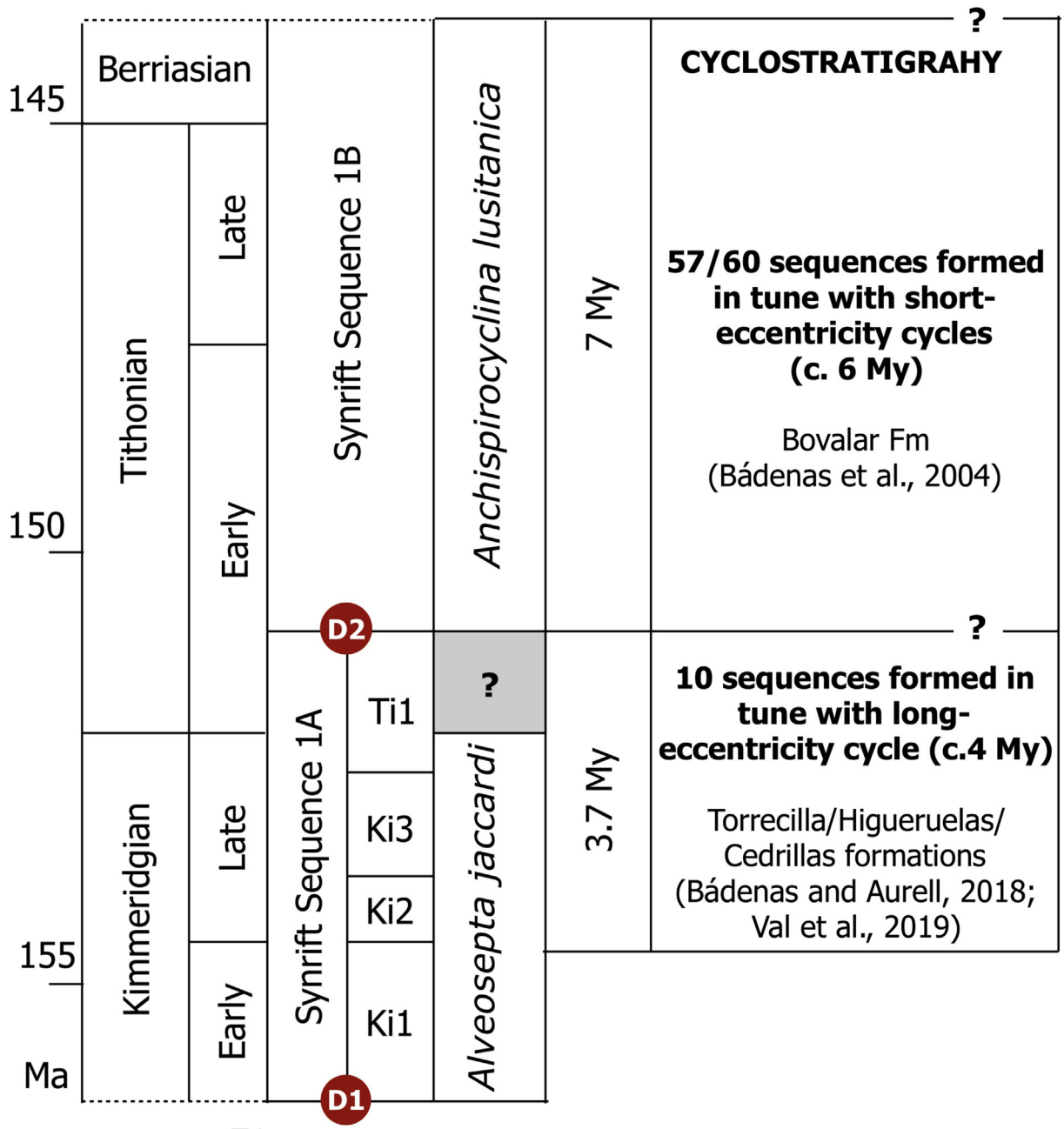

Fig. 11. Comparison between the stratigraphic calibration proposed in the present study and the cyclostratigraphic results obtained in previous works. Geological Time Scale from Ogg et al. (2016). For explanation see text.

formation of isolated grabens and half-grabens in discrete parts of the Galve subbasin. The upper boundary of synrift sequence 1C is a major unconformity related to synsedimentary tectonic reactivation around the Berriasian-Valanginian boundary, and there is an associated stratigraphic gap of variable amplitude that comprises the Valanginian and the Hauterivian.

In conclusion, the stratigraphic and tectono-sedimentary evolution of the central Iberian Rift System summarized here reinforces the observation that the sedimentation during the Berriasian was linked to the "Jurassic cycle", providing arguments that support the placement of the Jurassic-Cretaceous system boundary at the end of the Berriasian stage rather than at the Tithonian-Berriasian boundary.

Acknowledgements

Parts of the results of this work were presented on the occasion of the JK2018 conference in Geneva (see Granier B. (ed., 2019), *International Meeting around the Jurassic-Cretaceous Boundary*, Carnets de Géologie, Madrid, ISBN13: 978-2-916733-18-0, Book 2019/01 (CG2019_B01), 100 p). This research was subsidized by the Spanish Ministry of Science and Innovation (project CGL2017-85038-P) and by the Government of Aragón-FEDER 2014–2020 *Construyendo Europa desde Aragón* (Group E18: *Aragosaurus: Recursos Geológicos y Paleoambientales*). Authors would like to acknowledge the use of Servicio General de Apoyo a la Investigación-SAI, Universidad de Zaragoza. DC is supported by AGAUR

(Beatriu de Pinós Programme, BP2017). MMA is supported by a Q3 postdoctoral grant by FCT (grant number SFRH/BPD/113130/2015). Rupert Glasgow helped to improve the English of the manuscript. The authors are grateful for the reviews of Bruno Granier and André Strasser, and for the editorial work of Eduardo Koutsoukos whose useful suggestions have improved the quality of this paper.

References

Albrich, S., Bernaus, J.M., Boix, C., Caus, E., Martín-Closas, C., Salas, R., Vicedo, V., Villalonga, R., 2006. Caracterización bioestratigráfica y paleoambiental del Cretácico Inferior (Berriasiense-Barremiense) del macizo de Garraf (Cadena Costera Catalana). Revista Española de Micropaleontología 38 (2–3), 429–452.

Atrops, F., Meléndez, G., 1984. Kimmeridgian and Lower Tithonian from the Calanda-Berge area (Iberian Chain, Spain): Some biostratigraphic remarks. In: Proceedings 1st International Symposium on Jurassic Stratigraphy 2, pp. 377–392. Erlangen.

Aurell, M., 1990. El Jurásico Superior en la Cordillera Ibérica Central (provincias de Zaragoza y Teruel). Análisis de cuenca. PhD Thesis. Zaragoza University.

Aurell, M., Mas, R., Meléndez, A., Salas, R., 1994. El tránsito Jurásico–Cretácico en la Cordillera Ibérica: relación tectónica-sedimentación y evolución paleogeográfica. Cuadernos de Geología Ibérica 18, 369–396.

Aurell, M., Bádenas, B., Bello, J., Delvene, G., Meléndez, G., Pérez-Urresti, I., Ramajo, J., 1999a. El Calloviense y el Jurásico superior en la Cordillera Ibérica nororiental y la Zona de Enlace con la Cordillera Costero-Catalana, en los sectores de Sierra de Arcos, Calanda y Xerta-Paüls. Cuadernos de Geología Ibérica 25, 111–137.

Aurell, M., Bádenas, B., Bordonaba, A.P., 1999b. El Bathoniense– Kimmeridgiense (Jurásico Medio-Superior) en la región de Obón- Torre de las Arcas (Teruel). Geogaceta 25, 19–22.

Aurell, M., Robles, S., Bádenas, B., Quesada, S., Rosales, I., Meléndez, G., García-Ramos, J.C., 2003. Transgressive/regressive cycles and Jurassic palaeogeography of NE Iberia. Sedimentary Geology 162, 239–327.

Aurell, M., Bádenas, B., Ipas, J., Ramajo, J., 2010. Sedimentary evolution of an Upper Jurassic carbonate ramp (Iberian Basin, NE Spain). In: Buchem, F. van, Gerdes, K., Esteban, M. (Eds.), Reference Models of Mesozoic and Cenozoic Carbonate Systems in Europe and The Middle East, Stratigraphy and Diagenesis. Geological Society of London, pp. 87–109. Special Publication329.

Aurell, M., Bádenas, B., Gasca, J.M., Canudo, J.I., Liesa, C., Soria, A.R., Moreno-Azanza, M., Najes, L., 2016. Stratigraphy and evolution of the Galve sub-basin (Spain) in the middle Tithonian-early Barremian: implications for the setting and age of some dinosaur fossil sites. Cretaceous Research 65, 138–162.

Aurell, M., Soria, A.R., Bádenas, B., Liesa, C.L., Canudo, J.I., Gasca, J.M., Moreno-Azanza, M., Medrano-Aguado, E., Meléndez, A., 2018. Barremian synrift sedimentation in the Oliete sub-basin (Iberian Basin, Spain): palaeogeographical evolution and distribution of vertebrate remains. Journal of Iberian Geology 44, 285–308.

Aurell, M., Val, J., Bádenas, B., Liesa, C., 2019. Discordancias asociadas a una etapa de rift del final del Jurásico en el sector central de la Subcuenca de Galve (Aguilar del Alfambra, Teruel). Geogaceta 65 (in press). Q4

Bádenas, B., Aurell, M., 2001. Kimmeridgian palaeogeography and basin evolution of northeastern Iberia. Palaeogeography, Palaeoclimatology, Palaeoecology 168, 291–310.

Bádenas, B., Aurell, M., 2018. The down-dip preferential sequence record of orbital cycles in greenhouse carbonate ramps: examples from the Jurassic of the Iberian Basin (NE Spain). In: Montenari, M. (Ed.), Stratigraphy & Timescales volume 3: Astrochronology and Cyclostratigraphy. Elsevier, pp. 285–325.

Bádenas, B., Aurell, M., Rodríguez Tovar, F.J., Pardo-Izuzquiza, E., 2003. Sequence stratigraphy and bedding rhythms in an outer ramp limestone succession (Late Kimmeridgian, northeast Spain). Sedimentary Geology 161, 153–174.

Bádenas, B., Salas, R., Aurell, M., 2004. Three orders of regional sea-level changes control facies and stacking patterns of shallow carbonates in the Maestrat Basin (Tithonian-Berriasian, NE Spain). International Journal of Earth Sciences 93, 144–162.

Bádenas, B., Aurell, M., Gröcke, D.R., 2005. Facies analysis and correlation of high-order sequences in middle-outer ramp successions: variations in exported carbonate in basin-wide δ13Ccarb (Kimmeridgian, NE Spain). Sedimentology 52, 1253–1276.

Bádenas, B., Aurell, M., Gasca, J.M., 2018. Facies model of a mixed clastic-carbonate, wave-dominated open-coast tidal flat (Tithonian-Berriasian, north-east Spain). Sedimentology 65, 1631–1666.

Bover-Arnal, T., Moreno-Bedmar, J.A., Salas, R., Skelton, P.W., Bitzer, K., Gili, E., 2010. Sedimentary evolution of an Aptian syn-rift carbonate system (Maestrat Basin, E Spain): effects of accommodation and environmental change. Geologica Acta 8, 249–280.

Bover-Arnal, T., Moreno-Bedmar, J.A., Frijia, G., Pascual-Cebrian, E., Salas, R., 2016. Chronostratigraphy of the Barremian-Early Albian of the Maestrat Basin (E Iberian Peninsula): Integrating strontium-isotope stratigraphy and ammonoid biostratigraphy. Newsletters on Stratigraphy 49, 41–68.

Bryant, J.D., Jones, D.S., Mueller, P.A., 1995. Influence of fresh-water flux on $^{87}Sr/^{86}Sr$ chronostratigraphy in marginal marine environments and dating of vertebrate and invertebrate faunas. Journal of Paleontology 69, 1–6.

Campos-Soto, S., Cobos, A., Caus, E., Benito, M.I., Fernández-Labrador, L., Suarez-González, P., Quijada, E.I., Mas, R., Royo-Torres, R., Alcalá, L., 2017. Jurassic Coastal Park: a great diversity of palaeoenvironments for the dinosaurs of the Villar del Arzobispo Formation (Teruel, eastern Spain). Palaeogeography, Palaeoclimatology, Palaeoecology 485, 154–177.

Campos-Soto, S., Benito, M.I., Cobos, A., Caus, E., Quijada, E.I., Suarez- González, P., Mas, R., Royo-Torres, R., Alcalá, L., 2019. Revisiting the age and palaeoenvironments of the Upper Jurassic–Lower Cretaceous? dinosaur-bearing sedimentary record of eastern Spain: implications for Iberian palaeogeography. Journal of Iberian Geology. https://doi.org/10.1007/s41513-019-00106-y.

Canérot, J., 1974. Thèse Doctorat Sciences naturelles Toulouse. In: Recherches géologiques aux confins des chaines Ibériques et Catalanes (Espagne). Enadimsa.

Canérot, J., Cugny, P., Pardo, G., Salas, R., Villena, J., 1982. Ibérica Central y Maestrazgo. In: El Cretácico de España. Univ. Comp, Madrid, pp. 273–344.

Canudo, J.I., Gasca, J.M., Moreno-Azanza, M., Aurell, M., 2012. New information about the stratigraphic position and age of the sauropod *Aragosaurus ischiaticus* from the Early Cretaceous of the Iberian Peninsula. Geological Magazine 149 (2), 252–263.

Catuneanu, O., Galloway, W.E., Kendall, C.G.St.C., Miall, A.D., Posamentier, H.W., Strasser, A., Tucker, M.E., 2011. Sequence Stratigraphy: Methodology and Nomenclature. Newsletters on Stratigraphy 44 (3), 173–245.

Cepriá, J.J., Bádenas, B., Aurell, M., 2002. Evolución sedimentaria y paleogeografía del Jurásico superior (Kimmeridgiense superior- Titónico) en la Sierra de Arcos (Cordillera Ibérica). Cuadernos de Geología Ibérica 28, 93–106.

Cobos, A., Royo-Torres, R., Luque, L., Alcalá, L., Mampel, L., 2010. An Iberian stegosaurs paradise: the Villar del Arzobispo Formation (Tithonian-Berriasian) in Teruel (Spain). Palaeogeography, Palaeoclimatology, Palaeoecology 293, 223–236.

Colombié, C., Strasser, A., 2005. Facies, cycles and controls on the evolution of a keep-up carbonate platform (Kimmeridgian, Swiss Jura). Sedimentology 52, 1207–1228.

Colombié, C., Girauld, I.F., Schnyder, J., Götz, A., Boussaha, M., Aurell, M., Bádenas, B., 2014. Timing of sea level, tectonics and climate events during the uppermost Oxfordian (Planula Zone) on the Iberian ramp (northeast Spain). Palaeogeography, Palaeoclimatology, Palaeoecology 412, 17–31.

Díaz-Molina, M., Yébenes, A., 1987. La sedimentación litoral y continental durante el Cretácico Inferior. Sinclinal de Galve, Teruel. Estudios Geológicos (volumen extraordinario) 43, 3–21.

Fezer, R., Geyer, O.F., 1988. Der Oberjura von Calanda im nordöslichen Keltibericum (Provinz Teruel, Spanien). I Stratigrphie. Arbeiten aus dem Institut für Geologie und Paläontologie der Universität. Sttutgart 84, 207–237.

Finkel, R., 1992. Eine Ammoniten-Fauna aus dem Kimmeridgium des nord-östlichen Keltibericums (Spanien). Profil 3, 227–297.

García-Penas, A., Aurell, M., 2017. Tectonosedimentary evolution around the Jurassic–Cretaceous transition in Galve (Aguilar del Alfambra Formation, Teruel, Iberian Chain). Revista de la Sociedad Geológica de España 30, 79–90.

Gasca, J.M., Moreno-Azanza, M., Bádenas, B., Díaz-Martínez, I., Castanera, D., Canudo, J.I., Aurell, M., 2017. Integrated overview of the vertebrate fossil record of the Ladruñán anticline (Spain): evidence of a Barremian alluvial-lacustrine system in NE Iberia frequented by dinosaurs. Palaeogeography, Palaeoclimatology, Palaeoecology 472, 192–202.

Gautier, P.W., 1980. Memoria explicativa de la Hoja núm. 543 (Villarluengo). In: Mapa geológico de España 1:50.000, segunda serie. Instituto Geológico de España (IGME), Madrid.

Gautier, P.W., 1981. Memoria explicativa de la Hoja núm. 568 (Alcala de la Selva). In: Mapa geológico de España 1:50.000, segunda serie. Instituto Geológico de España (IGME), Madrid.

Geyer, O., Pelleduhn, R., 1979. Sobre la Estratigrafía y la facies espongiolítica del Kimmeridgiense de Calanda (provincia de Teruel). Cuadernos de Geología Ibérica 10, 67–72.

Granier, B., 2019. Dual biozonation scheme (benthic foraminifera and "calcareous" green algae) over the Jurassic-Cretaceous transition. Another plea to revert the system boundary to its historical Orbigny's and Oppel's definition. Cretaceous Research 93, 245–274.

Ipas, J., Aurell, M., Bádenas, B., Canudo, J.I., Liesa, C., Mas, J.R., Soria, A.R., 2007. Caracterización de la Formación Villar del Arzobispo al sur de Zaragoza (Titónico, Cordillera Ibérica). Geogaceta 41, 111–114.

Kleipool, L.,M., Reijmer, J.J.G., Bádenas, B., Aurell, M., 2015. Variations in petrophysical properties along a mixed siliciclastic carbonate ramp (Upper Jurassic, Ricla, NE Spain). Marine and Petroleum Geology 76, 329–343.

Liesa, C.L., Soria, A.R., Meléndez, A., 1996. Estudio preliminar sobre la tectónica sinsedimentaria del Cretácico inferior en el borde septentrional de la Cubeta de Aliaga (Cordillera Ibérica). Geogaceta 20 (7), 1707–1710.

Liesa, C.L., Soria, A.R., Casas, A., Aurell, M., Meléndez, N., Bádenas, B., Fregenal-Martínez, M., Navarrete, R., Peropadre, C., Rodríguez-López, J.P., 2019. The Late Jurassic–Early Cretaceous rifting stage at the central and eastern Iberian Basin. In: Quesada, C., Oliveira, J.T. (Eds.), The geology of Iberia: A Geodynamic Approach. Volume 5: The Alpine Cycle. Springer, Heidelberg.

Martín-Closas, C., 1989. Els caròfits del Cretaci Inferior de les conques periferiques del Bloc de l'Ebre. PhD thesis. University of Barcelona.

Martín-Closas, C., Salas, R., 1994. Lower Cretaceous Charophytes. Biostratigraphy and evolution in the Maestrat Basin (Eastern Iberian Ranges). In: Excursion Guidebook, VIII Meeting of the European Group of Charophyte Specialists, Barcelona, p. 89. Diagonal, Barcelona (ISBN 84-605-0645-2).

Please cite this article as: Aurell, M et al., Kimmeridgian–Berriasian stratigraphy and sedimentary evolution of the central Iberian Rift System (NE Spain), Cretaceous Research, https://doi.org/10.1016/j.cretres.2019.05.011

Martín-Closas, C., Salas, R., 1998. Lower Cretaceous Charophyte biozonation in the Maestrat Basin (Iberian Ranges, Spain). A reply to P.O. Mojon. Géologie Alpine 74, 97–110.

Martín-Closas, C., 2000. Els caròfits del Juràssic superior i el Cretaci inferior de la Península Ibèrica. Arxius de les Seccions de Ciències de l'Institut d'Estudis Catalans , Secció de Ciències i Tecnologia 125, 1–304 in Catalan with an abridged English version).

Mas, R., Alonso, A., Meléndez, N., 1984. La formación Villar del Arzobispo: un ejemplo de llanuras de mareas siliciclásticas asociadas a plataformas carbonatadas. Jurasico terminal (NW de Valencia y E de Cuenca). Publicaciones de Geología 20, 175–188.

Mas, R., García, A., Salas, R., Meléndez, A., Alonso, A., Aurell, M., Bádenas, B., Benito, M.I., Carenas, J.F., García-Hidalgo, J., Gil, J., Segura, M., 2004. Segunda fase de rifting: Jurásico Superior-Cretácico Inferior. In: Vera, J.A. (Ed.), Geología de España. SGE- IGME, Madrid, pp. 503–510.

McArthur, J.M., Howarth, R.J., Shields, G.A., 2012. Strontium isotope stratigraphy. In: Gradstein, F.M., Ogg, J.G., Schmitz, M.D., Ogg, G.M. (Eds.), A Geologic Time Scale 2012. Elsevier, Oxford, pp. 127–144.

Meléndez, G., Aurell, M., Atrops, F., 1990. Las unidades del Jurásico superior en el sector noroccidental de la Cordillera Ibérica: nuevas subdivisiones litoestratigráficas. Cuadernos de Geología Ibérica 14, 225–246.

Meléndez, A., Pardo, G., Pendón, J.G., Villena, J., 1979. Las facies terminales del Jurásico en el sector central de la Cordillera Ibérica. Cuadernos de Geología 10, 137–148.

Moliner, L., 2009. Ataxioceratinae (ammonitina) del Kimmeridgiense inferior en el NE de la provincia de Teruel (cordillera Ibérica oriental y Maestrazgo). PhD thesis. University of Granada.

Ogg, J.G., Ogg, G., Gradstein, F.M., 2016. A Concise Geologic Time Scale. Elsevier B.V.

Pérez-Urresti, I., Delvene, G., Meléndez, G., Ramajo, J., 1998. El Oxfordiense Superior y la posición del límite Oxfordiense-Kimmeridgiense en el sector de Tosos-Aguilón (Rama Aragonesa de la Cordillera Ibérica, España). Geogaceta 24, 251–254.

Peybernès, B., 1998. Larger benthic foraminifera. Columns for Jurassic chart of Mesozoic and Cenozoic sequence chronostratigraphic framework of European basins, by Hardenbol J, Thierry J, Farley MB, Jacquin T, De Gracianski PC, Vail PR (coordinators) Mesozoic and Cenozoic sequence chronostrati- graphic framework of European basins. In: Gracianski, P.C. de, Hardenbol, J., Jacquin, T., Vail, P.R. (Eds.), Mesozoic and Cenozoic Sequence Stratigraphy of European Basins. SEPM (Society for Sedimentary Geology). Special Publication 60, charts 7.

Querol, X., Salas, R., Pardo, G., Ardevol, L., 1992. Albian coal-bearing deposits of the Iberian Range in northeastern Spain. In: McCabe, J.P., Panish, J.T. (Eds.), Controls and distribution and quality of Cretaceous coals. Geological Society of America, pp. 193–208. Special Paper 267.

Ramajo, J., Aurell, M., 2008. Long-term Callovian–Oxfordian sea-level changes and sedimentation in the Iberian carbonate platform (Jurassic, Spain): possible eustatic implications. Basin Research 20, 163–184.

Ramalho, M.M., 1981. Note préliminaire sur le microfacies du Jurassique supérieur portugais. Communicações Serviços Geológicos de Portugal 67, 41–45.

Remane, J., 1991. The Jurassic-Cretaceous boundary: problems of definition and procedure. Cretaceous Research 12, 447–453.

Riveline, J., Berger, J.P., Feist, M., Martín-Closas, C., Schudack, M., Soulie-Märsche, I., 1996. European Mesozoic-Cenozoic charophyte biozonation. Bulletin de la Société géologique de France 167 (3), 453–468.

Salas, R., 1987. El Malm y el Cretaci inferior entre el Massis de Garraf i la Serra d'Espadà. Ph.D. Thesis. University of Barcelona.

Salas, R., Casas, A., 1993. Mesozoic extensional tectonics, stratigraphy and crustal evolution during the Alpine cycle of the eastern Iberian Basin. Tectonophysics 228, 33–55.

Salas, R., Martín-Closas, C., Querol, X., Guimerá, J., Roca, E., 1995. Evolución tectonosedimentaria de las cuencas del Maestrazgo y Aliaga-Penyagolosa durante el Cretácico inferior. In: Salas, R., Martín-Closas, C. (Eds.), El Cretácico inferior del Nordeste de Iberia. University of Barcelona, pp. 13–94.

Salas, R., Guimerà, J., Mas, R., Martín-Closas, C., Meléndez, A., Alonso, A., 2001. Evolution of the Mesozoic central Iberian rift system and its Cainozoic inversion (Iberian chain). Mémoires du Muséum national d'Histoire naturelle 186, 145–185.

Sames, B., 2011. Early Cretaceous *Theriosynoecum* Branson 1936 in North America and Europe. Micropaleontology 57 (4–5), 291–344.

Santos, A.A., Villanueva-Amadoz, U., Royo-Torres, R., Sender, L.M., Cobos, A., Alcala, L., Diez, J.B., 2018. Palaeobotanical records associated with the first dinosaur defined in Spain: Palynostratigraphy, taxonomy and palaeoenvironmental remarks. Cretaceous Research 90, 318–334.

Schudack, U., Schudack, M., 2012. Non-Cypridean Ostracoda from the Lower Cretaceous of the Iberian Chain (Spain). Neues Jahrbuch für Geologie und Paläontologie-Abhandlungen 266 (3), 251–271.

Sequero, C., Bádenas, B., Aurell, M., 2018. Facies mosaic in the inner areas of a shallow carbonate ramp (Upper Jurassic, Higueruelas Fm, NE Spain). Facies 64 (2), 9. https://doi.org/10.1007/s10347-018-0521-8.

Soria, A.R., Martín-Closas, C., Meléndez, A., Meléndez, N., Aurell, M., 1995. Estratigrafía del Cretácico inferior del sector central de la Cordillera Ibérica. Estudios Geol 51, 141–152.

Strasser, A., 1988. Shallowing-upward sequences in Purbeckian peritidal carbonates (lowermost Cretaceous, Swiss and French Jura Mountains). Sedimentology 35, 369–383.

Strasser, A., 2007. Astronomical time scale for the Middle Oxfordian to Late Kimmeridgian in the Swiss and French Jura Mountains. Swiss Journal of Geosciences 100, 407–429.

Strasser, A., Aurell, M., Bádenas, B., Meléndez, G., Tomás, S., 2005. From platform to basin to swell: orbital control on sedimentary sequences in the Oxfordian, Spain. Terra Nova 17, 407–413.

Tennant, P.J., Mannion, P.D., Upchurch, P., Sutton, M.D., Price, G.D., 2017. Biotic and environmental dynamics through the Late Jurassic–Early Cretaceous transition: evidence for protracted faunal and ecological turnover. Biological Reviews 92, 776–814.

Val, V., Bádenas, B., Aurell, M., Rosales, I., 2017. Cyclostratigraphy and chemostratigraphy of a bioclastic storm-dominated carbonate ramp (late Pliensbachian, Iberian Basin). Sedimentary Geology 355, 93–113.

Val, J., Aurell, M., Bádenas, B., Castanera, D., Subias, S., 2019. Cyclic carbonate–siliciclastic sedimentation in a shallow marine to coastal environment (latest Kimmeridgian–early Tithonian, Galve sub-basin, Spain). Journal of Iberian Geology 45, 195–222.

Vennin, E., Soria, A.R., Meléndez, A., Préat, A., 1993. Análisis secuencial durante el intervalo Barremiense–Aptiense en la Cubeta de Oliete. Cuadernos de Geología Ibérica 17, 257–283.

Wierzbowski, H., Anczkiewicz, R., Pawlak, J., Rogov, M.A., Kuznetsov, A.B., 2017. Revised Middle-Upper Jurassic strontium isotope stratigraphy. Chemical Geology 466, 239–255.

Appendix A. Supplementary data

Supplementary data to this article can be found online at https://doi.org/10.1016/j.cretres.2019.05.011.

Uncited reference

Díaz-Molina and Yébenes, 1987, Mas et al., 1984, Vennin et al., 1993. Q5